C.P. No. 1156

C.P. No. 1156

MINISTRY OF AVIATION SUPPLY

AERONAUTICAL RESEARCH COUNCIL

CURRENT PAPERS

A Further Wind Tunnel Investigation of Underwing Jet Interference

by

A. G. Kurn

Aerodynamics Dept., R.A.E., Farnborough

LONDON: HER MAJESTY'S STATIONERY OFFICE

1971

PRICE *70p* NET

U.D.C. 533.695.17 : 533.697.74 : 534.83

C.P. No. 1156*

April 1969

A FURTHER WIND TUNNEL INVESTIGATION OF UNDERWING JET INTERFERENCE

by

A. G. Kurn

Aerodynamics Dept., RAE, Farnborough

SUMMARY

Further experiments, to investigate the interference of the jet stream issuing from a high bypass ratio engine mounted below a wing, are described.

Tests have been made with a two-dimensional wing, and two nozzle shapes representing engines with different fan cowl lengths. A jet blowing from these nozzles produced negligible interference on the wing upper surface. However, a change in the lower surface pressure distribution occurred which was dependent only on the wing and nozzle geometry. This interference was dominated by a high suction peak, which appeared to be related to a region in the jet where the alternate expansion and compression waves were not uniformly spaced.

The tests were conducted mostly without an engine pylon. When a pylon was introduced the effect was reduced slightly, but the character of the interference remained unaltered.

An attempt was made to show the possibility of a wing altering the noise level by reflecting the sound from a jet. Schlieren pictures were taken with a spark source, but the expected phenomenon of aero-acoustic resonance was not found.

---

* Replaces R.A.E. Technical Report 69090 - A.R.C. 31505

CONTENTS

1 INTRODUCTION

The current design studies for large passenger aircraft, operating at high subsonic speeds, incorporate large-diameter engines, of high bypass ratio, mounted close to the undersurface of the wing. For such configurations there may be interference to the flow over the wing, not only from the displacement flow around the engine nacelle and the supporting pylon, but also from the jet efflux. Experiments were done, in the R.A.E. 2ft × 1·5ft transonic tunnel, to determine whether the latter effect was sufficiently serious to warrant representation of the jet flow on complete wind tunnel models[1]. The outcome of this investigation showed that, within the context of the test, representation of jet flow from a short fan cowl engine is unnecessary for nacelle positions that are typical for this type of aircraft, but, as would be expected, jet interference increased as the nacelle was moved closer to the wing.

These tests also showed that the change in pressure distribution on the lower surface of the wing, due to the interference by the jet, had a characteristic shape, which, apart from magnitude, was unaffected by jet pressure. This was a rather surprising result, as the jet stream without the wing present showed the usual lengthening of the spacing between the alternate expansion and compression waves as jet pressure was increased. It was not possible to observe the jet in the presence of the wing, as the wing was mounted across the schlieren beam, so the pattern of the pressure distribution remained unexplained.

A second series of experiments, the subject of this paper, were undertaken with the original nozzle supplying the jet stream but with another wing, mounted so that schlieren observations could be made. The object of this new investigation was to extend the programme of the previous tests, and, if possible, shed some light on the unexplained phenomenon. During the course of the experiments interest was transferred from short fan cowls to three-quarter length cowls, which were favoured by the aircraft designers for reasons of noise suppression. Consequently, an additional nozzle, representing a longer fan cowl and appreciably different in shape from the original, was included to give a comparison. Both of these nozzles are representative of an engine with a bypass ratio of about 5 to 1.

The tests on both nozzles were initially made without an engine pylon, and for current nozzle positions relative to the wing the interference was not

found to be large*. However, it was felt that a pylon might displace the jet stream nearer to the wing and appreciably increase the interference. To investigate this possibility three pylons have been tested with the nozzle representing the three-quarter length cowl.

2 EXPERIMENTAL DETAILS

2.1 The wing

A two-dimensional wing, was used for this investigation. It was mounted, inverted, across the tunnel, which had solid glass side walls and a slotted roof and floor, giving an open area ratio of 6%. The ends of the wing butted against the glass walls, and spigots from the position of maximum thickness passed through holes in the glass and were clamped to supports outside the tunnel working section. Sixty pressure holes in the surface around the wing were used to assess the jet interference, and these were arranged on a chord in line with the jet nozzle when testing was done without a pylon. For the tests with a pylon, the nozzle was rigged 0·2 in to one side to avoid covering these holes**.

Roughness strips to promote turbulence, near the leading edge of the wing, were tried, but were abandoned as they influenced the local pressures and made it difficult to assess the degree of interference by the jet stream. For all incidences at which the wing alone was tested, natural transition, as indicated by a sublimation technique using acenapthene, occurred at 0·70-0·75 c on the upper surface and 0·50-0·55 c on the lower surface.

The wing ordinates are presented in Table 1.

2.2 The nozzles

The jet air was supplied through a long tube, cantilevered from the tunnel contraction, on the end of which a nozzle shaped to represent the rear end of a fan jet engine was mounted. The arrangement of the apparatus (without a pylon) is shown in Fig.1, with details of the nozzles in Fig.2. Without a pylon, the nozzles were positioned with one of the three struts around the gas generator in the vertical plane through the nozzle axis on the side furthest from the wing, so that the jet issuing from the nozzle

---

*Some of the results of the experiments so far described, including those of Ref.1 were presented in a limited form at an AGARD Specialist Meeting, Paris, September 1968 [2]. Since then one or two small errors have come to light, so that where differences occur the results given in this Report are to be preferred.

** No pressure measurements were made at other spanwise stations as the lateral extent of jet interference on a wing is reported in Ref.1.

nearest the wing was completely unobstructed*. To hold a pylon in position, however, it was necessary to rotate the short nozzle (the only one tested with a pylon) so that one of the struts was in the vertical plane on the side nearest the wing. It can be seen in Fig.2 that the fan cowl is the same for both nozzles, and that the jet supply air, maintained at tunnel stagnation temperature approximately, is common to both the outer annular duct (i.e. the fan duct) and the inner duct (i.e. the gas generator). The ordinates for the two nozzles are listed in Table 2. For the sake of brevity the nozzle representing the short fan cowl engine is referred to as the 'long nozzle', and that representing the three-quarter length cowl as the 'short nozzle'.

The position of a nozzle relative to the wing was adjusted by altering the length of the tube, and by moving it vertically in the tunnel.

The long support tube developed a thick boundary layer at the nozzle. Part of this boundary layer was removed by suction through the slots shown in Figs.1 and 2 (see section 2.4).

2.3 The pylons

The pylons are presented in Fig.3: they were shaped by hand, and it is difficult to give dimensions other than plan measurements and a few thicknesses. Oil flow tests on the first pylon (A) suggested that the fan jet might be separating from the pylon at the very thick nose inside the fan cowl nozzle. In consequence pylons A* and B* were reduced in thickness in the fan stream, and made continuous with one of the three support struts joining the outer cowl to the inner nozzle. The pylons were tested only with the short nozzle. The support tube together with the nozzle and a pylon were displaced laterally to starboard by 0·20 in, so that the pressure holes on the wing lower surface were positioned in the junction of the wing and pylon, as mentioned in section 2.1.

2.4 Details of the test

Most of the experiments were made at a nominal free stream Mach number of 0·70 and a Reynolds number, based on wing chord, of $1{\cdot}33 \times 10^6$. To determine the effect of Mach number some testing was also done at $M_o = 0{\cdot}60$ and a Reynolds number of $1{\cdot}18 \times 10^6$. The stagnation pressure of the jet was varied from the free stream value to 2·9 times the free stream static pressure (i.e. from $H_J = H_o$ to $H_J = 2{\cdot}9\ p_o$). The former was selected as a basic condition to simulate a free flow nacelle as used in conventional model testing.

*In the previous investigation[1], pitot traverses across the fan duct exit did not detect the wakes from these struts, however, so any obstruction must have been small.

The two nozzles were tested at several positions relative to the wing, which are defined and tabulated in Fig.4. The datum case, had the nozzle positioned at $x_n = 0{\cdot}38\ D_e$ and $z_n = 0{\cdot}29\ D_e$. The conditions at which the nozzles were operated are tabulated below:-

H_J/p_o	H_J/H_o		C_T nett Long nozzle		C_T nett Short nozzle
M_o = 0·72 and 0·60	0·72	0·60	0·72	0·60	0·72
1·9	1·35	1·49	0·43	0·96	0·50
2·4	1·70	1·88	0·88	1·72	1·03
2·65	1·88				1·28
2·9	2·06	2·28	1·33	2·48	1·55

Reference area for C_T nett is $\frac{\pi}{4} D_e^2$ (see Fig.4).

It was found in the previous investigation[1] that the boundary layer varied in thickness around the tube supporting the nozzle. For that experiment the wing was placed adjacent to the side of the tube where the boundary layer was thinnest. In addition, confining the removal of the boundary layer to this region, by suction through 180° of the slots only around the circumference of the tube, resulted in a reasonably thin boundary layer wake between the jet stream and the wing. A complete description of the boundary layer suction system, which includes measurements of boundary layer thicknesses is given in Ref.3. For the tests reported here, with the wing positioned so that schlieren observations could be made, the natural boundary layer on the tube adjacent to the wing was considerably thicker than for the earlier tests. To keep the distortion of the wake to a minimum the natural boundary layer was thinned by suction around the complete circumference of the tube (360°). Although modifications to the bends in the suction ducts, through which the boundary layer air passed, gave an increase in mass flow of 30%, suction over 360° removed less of the boundary layer on the side of the tube nearest to the wing than when suction had previously been applied over 180° only. Estimates, based on the results of Ref.3, suggest that the boundary layer just upstream of the nozzle, on the side nearest the wing, had a displacement thickness of 0·066 in and a momentum thickness of 0·049 in. These thicknesses are about four times the values of the thinned boundary layer and 1·5 times the natural boundary layer of the tests described in Ref.1.

This thick boundary layer may be regarded as effectively reducing the momentum of the jet stream, thereby reducing the jet interference on the wing. To adjust the peak suctions of the interference pressures due to the jet stream on the lower surface of the wing (see section 3, and, as an example Fig.6b) to values comparable with those for the thinner boundary layer of Ref.1, it is estimated that for the datum position (z_n = 0·29 D_e) the peak suction must be raised by about 20%, and for z_n = 0·25 D_e an adjustment of about 40% is required: under some conditions such adjustments may well indicate supercritical flow. However, it must not be thought that this contradicts the finding of Ref.1, which concluded that interference from the jet flow was small for current positions of the engine. For these tests the majority of the wing incidence settings are lower than would normally be expected and, in consequence, undersurface pressures are also low. In addition the highest jet pressure ratio setting, H_J/p_o = 2·9, is in excess of that at which fan jet engines of this type are operated. Furthermore, it is shown in the results of these tests, that locally supercritical flow on the wing, caused by increasing the jet pressure, does not alter the pressure distribution very much apart from raising the level of the peak suction itself.

3 RESULTS

With the wing spanning the tunnel, Ref.4 predicted a correction of ΔM = -0·02 to the tunnel Mach number (M_o), and the pressure coefficients, based on M_o, that have been calculated from the wing pressures should be similarly corrected. However, no corrections have been made since the interference trends and the conclusions drawn from them do not depend on the precise Mach number. In any case, the tunnel corrections when the jet is blown are quite unknown.

Some of the results, shown in the figures, are pressure coefficient distributions over the wing. For the most part interest has been focussed on the changes in the distribution caused by jet blowing, and most of the results are shown as the difference in pressure coefficients (ΔC_{p_j}) when the jet is blowing at a given pressure ratio and when its total head is equal to the free stream value. i.e.

$$\Delta C_{p_j} = C_{p(H_J)} - C_{p(H_o)} \quad .$$

3.1 Jet blowing from the long nozzle

The tests on this nozzle were made to get some insight into the behaviour of the jet stream and its influence on the wing pressure field. To do this the nozzle was moved from its datum position to two other positions progressively nearer the wing. It must be pointed out, however, that no current design study has considered mounting engines as close to the wing as the two latter positions.

The previous tests with the long nozzle[1] suggested that the pressures on the upper surface of the wing were hardly influenced by the jet stream, only by the displacement flow around the nozzle and support tube. This is further confirmed by the pressure distributions shown in Figs.5a and 5b with the nozzle brought appreciably closer to the wing. Only in the extreme position, with the nozzle very nearly touching the wing ($z_n/D_e = 0{\cdot}03$) are the pressures significantly altered when the jet is blowing, and then only over the first 10% of the wing chord. It would appear that this local interference increases as Mach number is reduced (cf. Figs.5a and 5b); however, this may well be due to a very slight difference in the nozzle position for the two Mach numbers, although the setting in each case was nominally the same.

The wing-alone distributions on these graphs, and on Figs.6a and 7a, were obtained with the jet tube removed from a joint in the tunnel contraction and replaced by a boat-tail fairing. Later measurements on the wing alone (section 3.2) were done with the jet rig completely removed from the tunnel. The latter results indicated that the faired rig gave pressure distributions on the wing which have suctions over most of the upper surface that are too high by pressure coefficient increments of 0·02 to 0·04. On the lower surface (Figs.6a and 7a), over the maximum suction region, the distribution appears to be too low by about the same amount.

3.1.1 Interference on the wing lower surface

Figs.6a and 7a indicate the change in pressure distribution on the lower surface of the wing due to the presence of the nozzle and its support tube at Mach numbers of 0·72 and 0·60 respectively. This cannot be regarded as a true measure of the interference from the displacement flow around the tube, since transition on the wing, in the vicinity of the nozzle, was moved forward from 0·52 c to 0·25 c when $z_n/D_e = 0{\cdot}29$, and near to the leading edge for the two other nozzle positions.

The combined effect of the displacement flow around the tube and the movement of transition position is to move the suction peak at 0·40 c forward to 0·15 c approximately, and to reduce it appreciably, for the datum case (z_n/D_e = 0·29). For the two other nozzle positions, closer to the wing, the suction peak remains fixed in position but increases in magnitude.

The change from the zero thrust ($H_J = H_o$) pressure distributions, when jet pressure is increased, is shown by the plots of ΔC_{p_j} in Figs.6b-6d for M_o = 0·72, and Figs.7b-7d for M_o = 0·60. Initially, the effect of jet flow, *with the nozzle at the datum position (Figs.6b and 7b), is to produce a primary* suction peak at approximately 0·20 c, and a secondary suction peak further downstream. The primary peak increases in magnitude and moves slightly downstream as the jet pressure is increased, and as the nozzle is moved closer to the wing.

3.1.2 The effect of changing Mach number

The effect of changing Mach number is more clearly evident from Figs.8a-8c. Fig.8a shows that at M_o = 0·60 the jet pressure ratio has to be altered by an appreciably larger amount than at M_o = 0·72 to obtain a given change in the peak pressure coefficient. With the nozzle nearer to the wing, (Fig.8b), this large difference in the change of pressure ratio between the two Mach numbers has been reduced. A further point of interest, shown in Figs.8a and 8b, is that the pressure distribution at one Mach number can be adjusted by varying the jet pressure, until it is similar to that at the other Mach number with a different jet pressure ratio, even though in one case the flow may be locally supercritical and in the other completely subcritical (Fig.8b).

With the nozzle very close to the wing (Fig.8c), the lower surface becomes one boundary of the jet stream (see section 3.1.3) and it would be expected that the pressure distribution will be largely unaffected by changes in the free stream Mach number. The level of the suction peaks for the two Mach numbers confirm this, as in each case taking $H_J = 2{\cdot}4\ p_o$ as an example, a pressure has been reached which is equivalent to a local Mach number of 1·88 approximately.

3.1.3 Schlieren studies

The almost constant pattern of the interference pressure distribution on the lower surface of the wing does not show the alternate expansion and compression waves that appear in the jet stream of the nozzle alone (Fig.9);

in particular there is no indication in the wing pressures of the increase in the spacing of these waves as jet pressure is increased. The reason for this is partially explained in Fig.10 where it can be seen that although the shocks in the jet on the far side of the nozzle are spaced in a conventional manner, becoming further apart as jet pressure increases, those near the wing have a very different pattern and remain substantially unaltered. This leads to an unsymmetrical flow distribution in the jet, which can be clearly seen further downstream.

The jet stream near the wing is free of shocks for more than 20% of the wing chord, and remain so as Mach number is altered and as the nacelle-wing spacing is reduced. The primary suction peak on the wing pressure distribution occurs just downstream of the narrowest part of the gap between the nozzle and the wing.

The photographs of Fig.10, which show the nozzle at the three positions, illustrate how the jet stream influences the wing pressure distribution. When $z_n/D_e = 0{\cdot}29$ a channel of free stream air between the wing and the jet may clearly be seen. With the nozzle nearest the wing ($z_n/D_e = 0{\cdot}03$), however, it is obvious that the undersurface of the wing is completely immersed in the jet stream. As might be expected, in the mid-position, ($z_n/D_e = 0{\cdot}16$), transitional flow conditions between these extremes apply. Due to a more direct influence of the jet stream the character of the pressure distribution changes (Fig.6c), particularly at the higher jet pressure ratios.

3.2 Jet blowing from the short nozzle

The tests on this nozzle were made with the vertical distance between the wing and the nozzle confined to two values more representative of current aircraft designs. The effects of moving the nozzle in a streamwise direction and of changing the angle of incidence of the wing have also been explored.

With the wing at two different angles of incidence Figs.11a and 11b show that, apart from the displacement effect of the nozzle, there is negligible interference on the wing upper surface due to jet pressure and the position of the nozzle.

3.2.1 Interference on the wing lower surface

Figs.12a-12d and Figs.13a-13d show the interference effects on the wing lower surface for the two vertical positions and the three streamwise positions of this nozzle. The wing incidence during these tests was $0{\cdot}7°$, and the flow under all conditions with one exception was everywhere subsonic.

Figs.12a and 13a show the 'displacement effect' of the nozzle and its support tube on the pressure distribution for the wing alone (see section 3.1.1). The suction peak, at 0·40 c, is appreciably reduced, but not displaced, as was the case for the long nozzle. As the nozzle is moved in a streamwise direction towards the wing a second suction peak at 0·04 c grows in magnitude, accompanied by a reduction of the peak at 0·40 c. The position of the highest pressure between the two suction peaks coincides with the end of the nozzle. Comparing the two figures it can be seen that the vertical movement of the nozzle has no noticeable effect on the pressure distributions.

Figs.12b and 13b show the interference pressure distribution with jet flow and with the nozzle at the datum position, $x_n/D_e = 0·38$. Again, although appreciably different from the long nozzle, the interference curves have a characteristic shape, with a peak suction, which, apart from an initial upstream movement, moves downstream as jet pressure ratio is increased. For the closer position of the nozzle to the wing, Fig.13b, the interference is increased, and it is at this position with the jet pressure-ratio of 2·9 that the local velocity at 0·40 c is slightly supersonic. It is to be noted that with the nozzle in this position the suction peak of the interference curves, particularly for $H_J = 2·9\ p_o'$, nearly coincides in position on the wing chord with the suction peak of the zero-thrust distribution ($H_J = H_o$).

It should be noted that as the nozzle is moved upstream and downstream by 8·3% c (Figs.12c and 12d and Figs.13c and 13d), the peaks of the interference curves move only about 5% c, and they also decrease in magnitude. As expected, interference increases as nacelle-wing spacing is reduced for these two positions.

3.2.2 The effect of wing incidence

The effect of wing incidence on the pressures on the wing lower surface with the nozzle at the datum position, is shown in Figs.14a-14e. The 'displacement effect' due to the nozzle and its support tube (see section 3.1.1) is shown in Fig.14a. With the nozzle in position it can be seen that as incidence is increased the suction peak at 0·40 c is reduced, as also, but to a greater extent, is the peak at 0·04 c. Figs.14b-14e show that the incremental pressure distributions due to the interference from the jet stream are not altered in character or position on the wing as incidence is varied. There is, however, a decrease in the level of the suction peaks as the angle of incidence is increased, except at the highest incidence of 2·3°, where the peak has

risen slightly. Due to the angular rotation of the wing about its leading edge the wing moves nearer to the jet as incidence increases, and is therefore subject to a larger interference effect producing higher suction peaks. It is possible that this effect of incidence becomes dominant for $\alpha > 2{\cdot}0$ and explains the increase in the levels of the suction peaks observed between $\alpha = 1{\cdot}9°$ and $2{\cdot}3°$. It is to be noted that the suction peaks are approximately coincident in position at 0·40 c with the peaks for zero thrust (Fig.13a), and, as already implied, as the magnitude of the basic peak decreases so does the magnitude of the interference peak. This trend in the peak value of the interference curves is somewhat similar to the result shown when the nozzle was moved in a streamwise direction and shows that interference is dependent in some way on the magnitude and distribution of the local velocities on the wing at zero thrust. Attempts to analyse the test results to find a simple law for this dependence, however, have not been successful.

3.2.3 Schlieren studies

Although there is an appreciable difference in the afterbody shapes of the two nozzles, Fig.15 shows that, as for the long nozzle (Fig.10), the pattern of the shock waves on the side of the short nozzle nearest the wing does not change to any noticeable extent as the several parameters are varied. The photographs with the schlieren knife-edge horizontal show that the jet stream is deflected towards the wing as incidence is decreased. The photographs with the schlieren knife-edge vertical show a change in the shock wave pattern downstream of the nozzle. The first compression region, in front of which the suction peak occurs on the wing, changes shape, and is more dense at $\alpha = 0{\cdot}3°$.

The significant difference between the interference pressure distributions for the two nozzles, is that whilst for the long nozzle the suction peak on the wing occurs within the length of the channel formed between the nozzle and the wing, for the short nozzle it is downstream of the nozzle. Comparing the shock systems behind the two nozzles (cf. Figs.10 and 15), it can be seen that although the shock pattern behind the long nozzle expands with jet pressure in a more or less conventional manner, the first shock or compression region downstream of the short nozzle remains stationary. It is just in front of this shock that the suction peak on the wing with the short nozzle occurs, and the fixed character of the interference pressure distribution is obviously associated in some way with the fixed position of the first shock in the jet.

3.3 Pylons

Three pylons were tested with the short nozzle: they are described in section 2.3 and illustrated in Fig.3.

3.3.1 Interference on the wing lower surface

Wing lower surface pressure coefficient distributions with all three pylons, at zero thrust conditions, are compared in Fig.16a. There is no great difference between these distributions, and the effect of the pylons can be seen by comparing this figure with Fig.14a. The suction peak near the front of the wing has risen due to the combination of the pressure gradients from the leading edges of both wing and pylon, whilst the peak at 0·40 c has decreased slightly. The somewhat curious distribution of the curve for pylon B* from 0·10 c to 0·20 c may be due to irregularities in the wing-pylon junction, as it was not possible to make the pylon a perfect fit on the wing near the leading edge.

The effect of jet blowing is shown in Figs.16b-16d. The flow over pylon A, as shown by a surface oil technique, suggested that in the fan jet stream the flow was not attaching to the pylon. To rectify this the pylon was locally reduced in thickness and modified inside the fan duct, as described in section 2.3; the modified shape then became pylon A*. The jet interference due to the alteration can be seen from Figs.16b and 16c. The modification has caused an increase in the suction peaks, and the trailing edge pressures suggest a small separation at the rear of the wing. With the nozzle closer to the wing and pylon B* fitted (which apart from the reduced span was similar to pylon A*) the jet interference, as would be expected, is increased, (Fig.16d). For this case no trailing edge separation was observed.

The effect of jet interference due to pylon A* can be inferred by comparing the pylon case at $\alpha = 0·5°$ (Fig.16c) with the results without a pylon at incidences of $0·3°$ and $0·7°$ (Figs.14b and 14c). The character of the interference due to the jet stream is not altered by the presence of the pylon, which appears to provide a favourable interference by reducing the suction peaks, although it must be remembered that the pressure holes on the wing are now offset by 0·20 in (see section 2.3). In addition, with pylon B* at $z_n/D_e = 0·23$, the flow over the wing is subsonic, even at $H_J/p_o = 2·9$ (Figs.16a and 16c, $C_p^* = 0·70$), whereas without a pylon at $z_n/D_e = 0·25$ and $\alpha = 0·7°$ the flow at the suction peak is slightly supercritical at $H_J/p_o = 2·9$ (Figs.13a and 13b).

3.3.2 Flow studies

By suitably illuminating the model with front lighting it was possible to produce photographs of oil-flow over the pylon in conjunction with changes in air density shown up by the schlieren beam. Two such photographs with pylon A* and pylon B* are presented in Figs.17a and 17b. Significant features of the flow on the pylons are, the very curved path of the free-stream air around the wing leading edge, and the upflow along the pylon onto the wing near the pylon trailing edge. The jet from the fan nozzle is attached to the pylon, and follows the shape of the thinned section provided for it to the end of the centre nozzle, where it is deflected by the expansion from this nozzle*. The first shock in the fan jet stream on the side of the nozzle furthest from the wing can be traced around the nozzle by the line of oil left by a small separation bubble. This shock moves progressively forward by a small amount as circumferential distance from the pylon is reduced; its position is shown up in the oil pattern on the side of pylon A*. Also present, but not clearly shown in the photographs, is some downwash on the fan cowl, which increases as the nozzle is moved closer to the wing.

Prior to the investigation it was felt that the growth of the boundary layer associated with a pylon might attract the jet stream closer to the wing (by analogy with the Coanda effect whereby a jet attaches to an adjacent surface) and so increase the interference. The pressure distributions, however, suggest that interference is reduced (section 3.3.1). Schlieren pictures with and without a pylon are compared in Fig.18a, and measurements of the jet stream boundary nearest the wing show that with the pylon present this boundary is further from the wing than the corresponding boundary without a pylon. Further study of these photographs gives rise to speculation on the cross-sectional shape of the jet. Unfortunately pressure measurements across the jet were not made during this experiment, but unpublished data obtained behind an elliptic and a rectangular nozzle have shown that any initial asymmetry in the flow seems to be magnified as the jet extends downstream. In the present case it seems plausible that the wake of the pylon (including the support strut inside the nozzle) could lead to a distortion of the jet similar to that sketched in Fig.18b. The effective movement of the jet away from the wing would explain the reduced interference.

---

*The dark region on the thin part of the pylon just behind the inner nozzle (Fig.17a) is a surface blemish filled with plastic material. It is not associated with the oil flow.

4 JET NOISE REFLECTED FROM A WING

In addition to the main investigation of jet interference it was thought worthwhile to do a limited exploration to show whether the presence of a wing might alter the noise level by reflecting the noise from a jet placed near it.

It is well known that, under some conditions, a phenomenon known as 'jet screech' can occur. This is an aero-acoustic resonance in which small disturbances at the nozzle, in the jet boundary, are amplified as they pass downstream, eventually causing instability of the jet giving rise to sound waves which travel upstream in the surrounding air to initiate further disturbances at the nozzle. In a previous investigation in the R.A.E. 2ft x 1·5ft tunnel[5], with a nozzle surrounded by an annular base, it had been possible to photograph the sound waves due to resonance by using a short duration spark as the light source of the schlieren system (see Fig.19a). This same light source was again used to take a large number of photographs of the short nozzle alone, and of the nozzle with the wing in position. The conditions covered a range of Mach numbers from 0·5 to 0·8, and jet pressure ratios from 2·4 to 3·5. It was thought that some of the photographs of the nozzle alone would show the sound waves related to the resonance phenomenon, and at the same conditions with the wing present might show these waves being reflected from the wing. However, it was not possible, with the short nozzle, to produce this aero-acoustic resonance. Fig.19b is a typical result, with and without the wing present. A large number of weak random waves are just visible, but they are nothing like the well defined waves of Fig.19a which indicate a discrete frequency of large amplitude.

5 CONCLUSIONS

Tests have been made with a two-dimensional wing, and two nozzle shapes representing an engine of bypass ratio approximately 5:1, with a short fan cowl and a three-quarter length fan cowl respectively. These tests were designed to give information applicable to a twin-engined, short-range transport aircraft, with moderate wing sweep.

The investigation is an extension of the experiments described in Ref.1, but with the boundary layer surrounding the nozzles appreciably thicker (see section 2.4). Adjusting the results of these tests to bring them into line with those for the thinner boundary layer suggests that for some conditions, where the nozzle is placed a representative distance from the wing, locally supersonic flow will occur on the lower surface of the wing. However, it must

not be thought that this contradicts the findings of Ref.1, which concluded that the interference from the jet flow was small. For these tests the majority of the wing incidence settings are lower than would normally be expected, and in consequence undersurface pressures are also low. In addition the highest jet pressure ratio setting, $H_J/p_o = 2{\cdot}9$, is in excess of that at which fan jet engines of this type are operated.

It is evident that there is a complex interaction between the jet and wing flows, and it would be interesting to try and examine the region between the nozzle and the wing in detail. However, it has not been possible to do this, and attention has been focussed on the more practical effects on the wing pressure distribution of varying jet pressure, nozzle position and wing incidence. A limited examination of the flow field has been made by schlieren observations.

The tests were conducted mostly without an engine pylon, and when a pylon was introduced the character of the interference remained unaltered.

The main results and conclusions are listed below:-

(1) A jet stream issuing from an engine nozzle produces negligible interference on the wing upper surface unless the vertical position of the nozzle brings the edge of the jet stream extremely close to the wing leading edge.

(2) The change in the pressure distribution on the wing lower surface, due to the jet stream, has a characteristic shape depending on the wing and nozzle geometry. It is dominated by the presence of a high suction peak.

(3) The magnitude of the interference increases as wing incidence is reduced, as jet pressure is increased, and as the nozzle is moved closer to the wing. A change in character becomes apparent by $z_n/D_e = 0{\cdot}20$ approximately, depending on jet pressure ratio, the wing becoming more directly influenced by the jet.

(4) With the nozzle very close to the wing, the flow over the lower surface of the wing in the jet stream is independent of the free stream Mach number.

(5) The pressure distribution over the wing lower surface at one Mach number can be made similar to that at another Mach number by suitably adjusting the jet pressure. This similarity in distribution can be achieved even although in one case the flow may be locally supersonic, and in the other completely subsonic.

(6) The alternate expansion and compression waves in the jet from the fan nozzle, on the side furthest from the wing, are spaced in a conventional manner and expand downstream as jet pressure is increased. The flow from the fan nozzle near to the wing has a very different pattern and remains substantially unaltered with change of jet pressure. This leads to an unsymmetrical flow distribution in the jet stream.

(7) The magnitude of the interference suction peak due to the jet stream appears to depend on the pressure distribution over the wing at zero thrust. Moving the nozzle with the short afterbody (three-quarter length cowl) in the free stream direction does not alter the position of a low pressure peak that occurs on the wing at zero thrust. The suction peak that is superimposed by jet blowing does move with movement of the nozzle; it also varies in magnitude, becoming a maximum when the two peaks coincide in position.

(8) The interference suction peak is positioned on the wing within the length of the long afterbody, but downstream of the short afterbody. In both cases it appears to be related to a region where the alternate expansion and compression waves in the jet stream are not uniformly spaced.

(9) Positioning a pylon between the wing and the nozzle reduces the interference from the jet stream. This appears to move the jet stream away from the wing, which would account for the reduced interference, although this apparent movement may well be due to a change in the cross-sectional shape of the jet.

Table 1

AEROFOIL ORDINATES

Wing RAE 2806

(All dimensions in inches)

x	z Upper surface	z Lower surface	x	z Upper surface	z Lower surface
0	0	0	2.52	0.3667	-0.3463
0.06	0.0743	-0.0794	2.64	0.3673	-0.3378
0.12	0.1099	-0.1092	2.78	0.3679	-0.3272
0.18	0.1314	-0.1344	2.88	0.3674	-0.3160
0.24	0.1476	-0.1547	3.00	0.3656	-0.3034
0.30	0.1632	-0.1703	3.12	0.3634	-0.2899
0.36	0.1778	-0.1862	3.24	0.3599	-0.2752
0.42	0.1916	-0.1999	3.36	0.3553	-0.2587
0.48	0.2045	-0.2119	3.48	0.3496	-0.2431
0.54	0.2153	-0.2241	3.60	0.3419	-0.2271
0.60	0.2253	-0.2344	3.72	0.3336	-0.2096
0.66	0.2355	-0.2445	3.84	0.3245	-0.1932
0.72	0.2446	-0.2537	3.96	0.3141	-0.1745
0.78	0.2533	-0.2631	4.08	0.3026	-0.1565
0.84	0.2611	-0.2709	4.20	0.2906	-0.1389
0.90	0.2679	-0.2794	4.32	0.2769	-0.1221
0.96	0.2754	-0.2872	4.44	0.2628	-0.1060
1.02	0.2822	-0.2937	4.56	0.2481	-0.0887
1.08	0.2889	-0.3004	4.68	0.2323	-0.0740
1.14	0.2950	-0.3065	4.80	0.2160	-0.0593
1.20	0.3002	-0.3114	4.92	0.1988	-0.0474
1.32	0.3116	-0.3225	5.04	0.1813	-0.0347
1.44	0.3213	-0.3314	5.16	0.1624	-0.0236
1.56	0.3300	-0.3387	5.28	0.1439	-0.0135
1.68	0.3375	-0.3449	5.40	0.1240	-0.0055
1.80	0.3438	-0.3502	5.52	0.1036	0.0003
1.92	0.3499	-0.3545	5.64	0.0817	0.0051
2.04	0.3546	-0.3556	5.76	0.0589	0.0070
2.16	0.3582	-0.3555	5.88	0.0327	0.0042
2.28	0.3617	-0.3547	6.00	-0.0018	-0.0050
2.40	0.3645	-0.3509			

Table 2

NOZZLE ORDINATES

See also Fig. 2

(All dimensions in inches)

Outer cowl			Long nozzle (inner)			Short nozzle (inner)		
x_J	Inside diameter	Outside diameter	x_J	Inside diameter	Outside diameter	x_J	Inside diameter	Outside diameter
-5·5	1·64	2·49	-3·5	0·89	0·89	-3·35	0·95	0·95
-4·5	1·70	↓	-3·375	0·80	1·02	-3·25	0·90	1·09
-4·0	1·75		-3·25	↓	1·09	-3·0	↓	1·21
-3·75	1·79		-3·0		1·21	-2·75		1·32
-3·5	1·84		-2·75		1·32	-2·5		1·39
-3·25	1·92		-2·5		1·39	-2·375		1·40
-3·0	2·00		-2·375		1·40	-1·0		1·40
-2·75	2·08	↓	-1·0		1·40	-0·625		1·54
-2·48	2·13	2·492	-0·625		1·54	-0·25		1·61
-2·28	2·14	2·493	-0·25		1·68	0		1·610
-2·08	↓	2·490	-0·02		1·677	0·10		1·599
-1·88		2·479	0·08		1·677	0·20		1·577
-1·68		2·464	0·18		1·676	0·30		1·545
-1·48		2·445	0·28		1·674	0·40		1·504
-1·28		2·421	0·38		1·668	0·50		1·457
-1·08		2·391	0·48		1·657	0·60		1·410
-0·88		2·358	0·58		1·644	0·70	0·90	1·362
-0·68		2·322	0·68		1·629	0·80	↑	1·314
-0·48		2·285	0·78		1·612	0·90		1·266
-0·28		2·247	0·88		1·594	1·00	linear	1·218
-0·08		2·201	0·98		1·574	1·10		1·170
0	2·14	2·169	1·08		1·552	1·20	taper	1·122
			1·18		1·528	1·30		1·074
			1·28		1·501	1·40		1·027
			1·38		1·473	1·50		0·979
			1·48		1·441	1·60		0·931
			1·58		1·408	1·70	↓	0·883
			1·68		1·372	1·775	0·826	0·840
			1·78		1·333			
			1·88		1·293			
			1·98		1·251			
			2·08	↓	1·209			
			2·18	0·80	1·166			
			2·28	↑	1·122			
			2·38		1·079			
			2·48	linear	1·035			
			2·58		0·991			
			2·68		0·947			
			2·78		0·903			
			2·88		0·859			
			2·98		0·815			
			3·08	taper	0·768			
			3·21	0·73	0·751			

SYMBOLS

c	wing chord
C_p	pressure coefficient
C_p^*	critical pressure coefficient (for which M = 1)
ΔC_{p_J}	incremental change in pressure coefficient due to jet stream
$C_{T\ nett}$	nett thrust coefficient
D_e	diameter of fan cowl at fan nozzle exit
H_J	stagnation pressure of jet stream
H_o	stagnation pressure of free stream
M_o	free stream nominal Mach number
p_o	static pressure in free stream
x	distance along wing chord from the leading edge
x_J	streamwise nozzle ordinate measured from the fan nozzle exit
x_n	streamwise distance of wing leading edge from the fan nozzle exit
y_n	vertical distance from the wing leading edge to the nozzle centre-line
z_n	vertical distance from the wing leading edge to the nearest point on the fan cowl trailing edge
α	geometric wing incidence measured from the horizontal plane

REFERENCES

No.	Author	Title, etc.
1	D.J. Raney A.G. Kurn J.A. Bagley	Wind tunnel investigation of jet interference for underwing installation of high bypass ratio engines. A.R.C. C.P.1044 (1968)
2	J.A. Bagley	Wind tunnel experiments on the interference between a jet and a wing at subsonic speeds. R.A.E. Technical Memorandum Aero 1079 (1968) AGARD C.P. 35, Paper No.22 (1968)
3	A.G. Kurn	A suction control system for the boundary layer developed along a cylinder. R.A.E. Technical Memorandum Aero 1090 (1968)
4	H.C. Garner (Ed.)	Subsonic wind tunnel wall corrections. Chapter 6: Wall interference in tunnels with ventilated walls. AGARDograph 109, October 1966
5	J.E. Rossiter A.G. Kurn	Wind tunnel measurements of the effect of a jet on the time average and unsteady pressures on the base of a bluff afterbody. A.R.C. C.P.903 (1965)

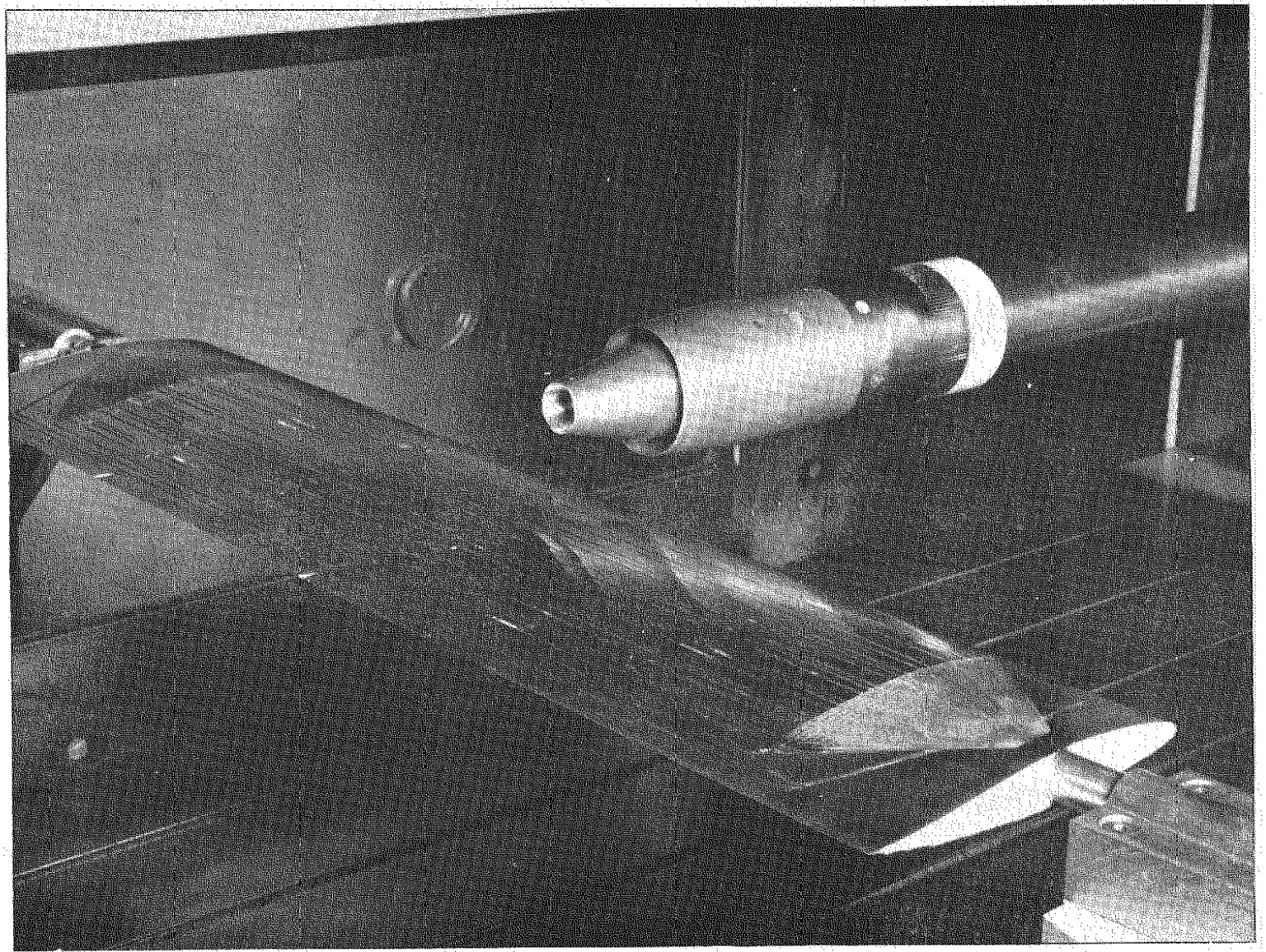

Fig.1 Model in tunnel

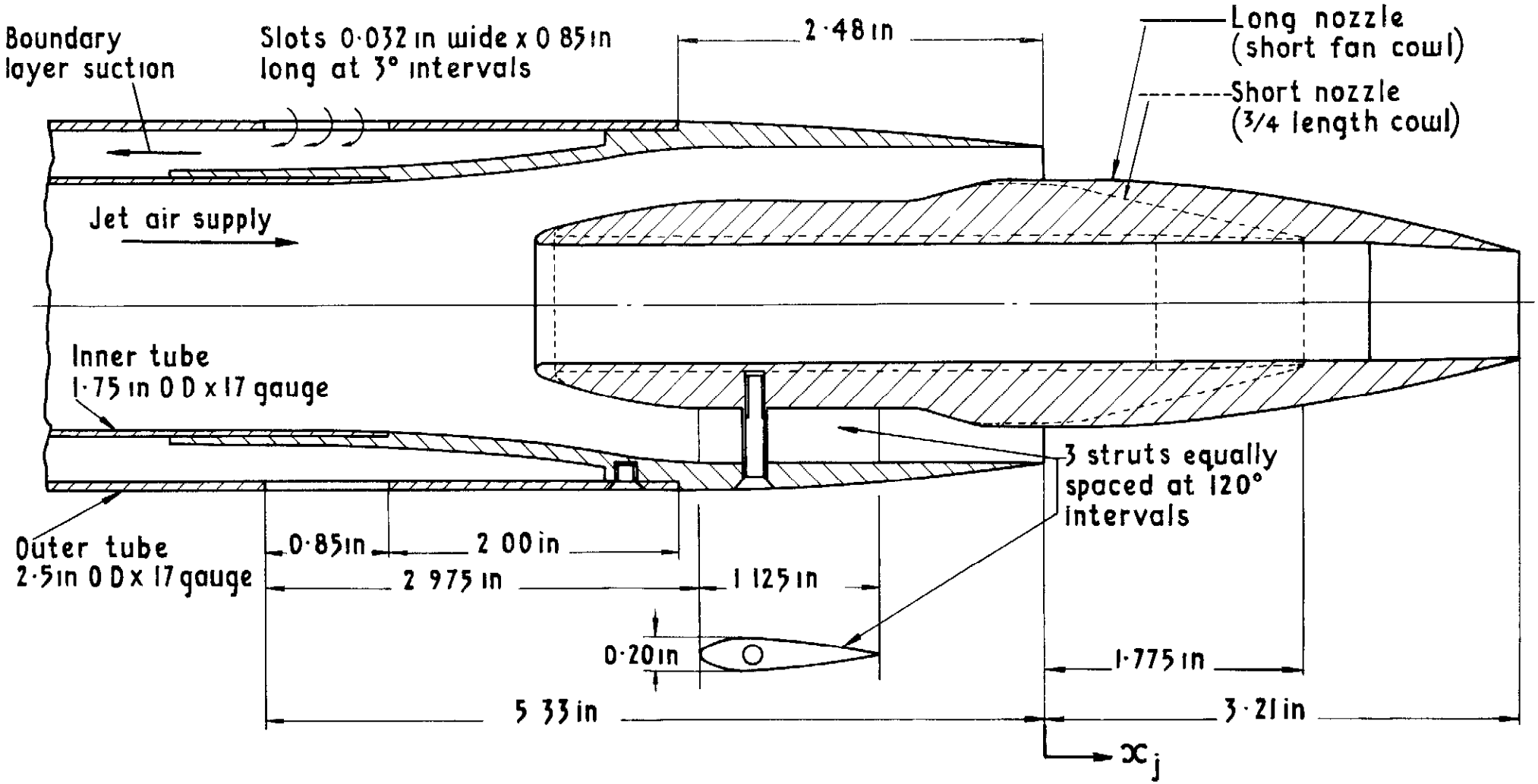

Fig. 2 Nozzle design

See also Table 2

All pylons have a maximum thickness of 0·45 in at the cowl junction 1·2 in back from the most forward part of the leading-edge. The thickest part of the pylons at the wing junction is 0 40 in just behind the wing leading-edge. A linear taper is maintained to the trailing edge of the pylons

Pylon A—Short nose entering fan nozzle The thickness of this nose is 0·386 in at the fan-cowl junction and 0·314 in at the gas-generator junction

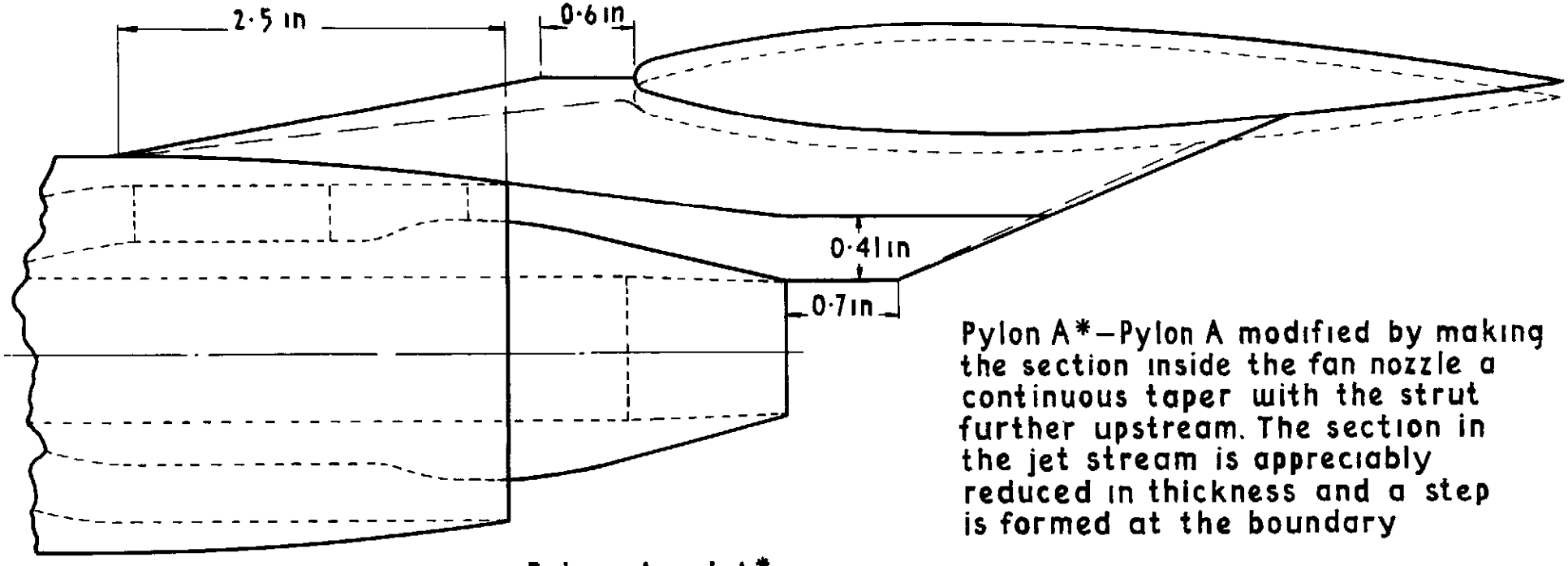

Pylon A*—Pylon A modified by making the section inside the fan nozzle a continuous taper with the strut further upstream. The section in the jet stream is appreciably reduced in thickness and a step is formed at the boundary

Pylon B*—Similar to Pylon A* with Z_n reduced (See fig 4)

Fig. 3 Pylons

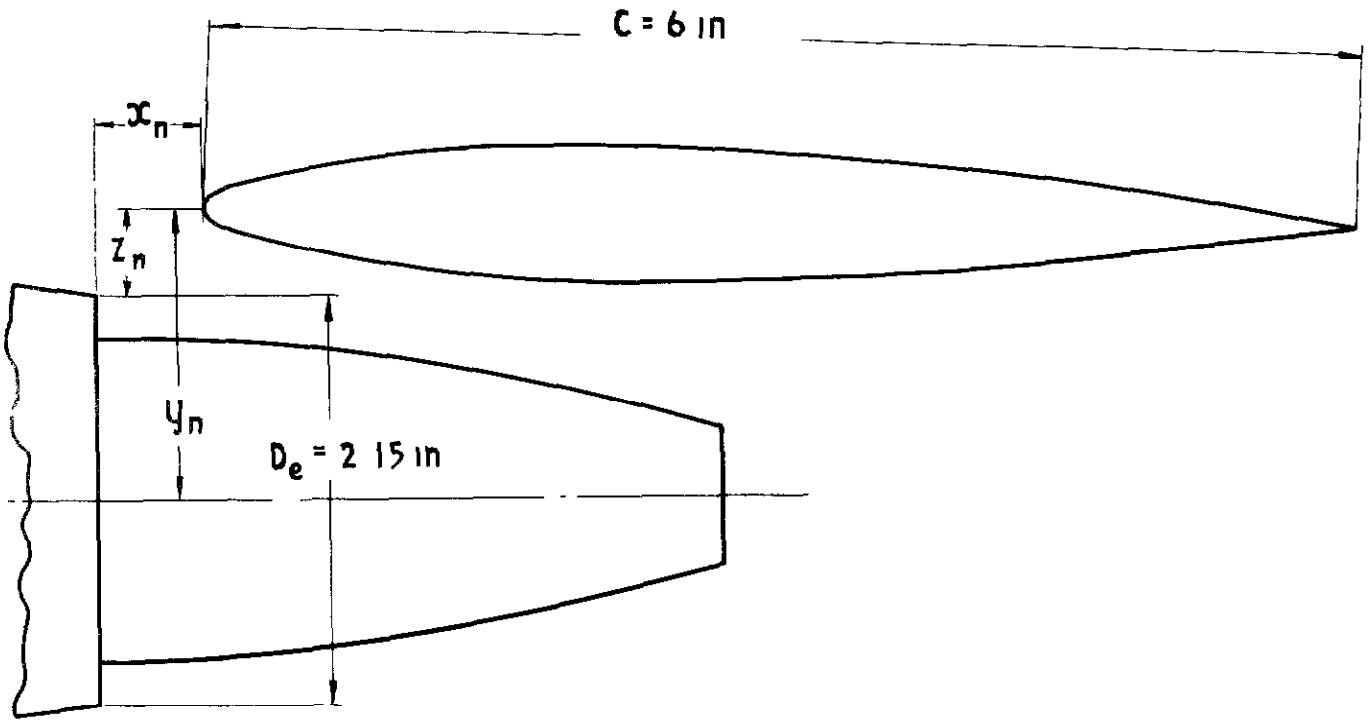

M_o	$\alpha°$	x_n/D_e	y_n/D_e	z_n/D_e
Long inner nozzle (Short fan cowl)				
0 72 and 0·60	1 3	0·38	0·79	0·29
	1 3	0·38	0·66	0·16
	1·3	0·38	0·53	0·03
Short inner nozzle (3/4 length fan cowl)				
0·72	0 7	0·61	0·79	0·29
	0·7	0·38	0·79	0 29
	0·7	0·15	0·79	0·29
	0·7	0·61	0·75	0·25
	0·7	0·38	0·75	0·25
	0·7	0·15	0·75	0·25
	0·3	0·38	0·79	0·29
	1 9	0 38	0·79	0·29
	2 3	0·38	0·79	0·29
Pylon A	0·5	0·38	0·79	0·29
Pylon A*	0·5	0·38	0·79	0·29
Pylon B*	0·5	0·38	0·73	0·23

* Thin section behind fan nozzle (See fig 3)

Fig 4 Test programme

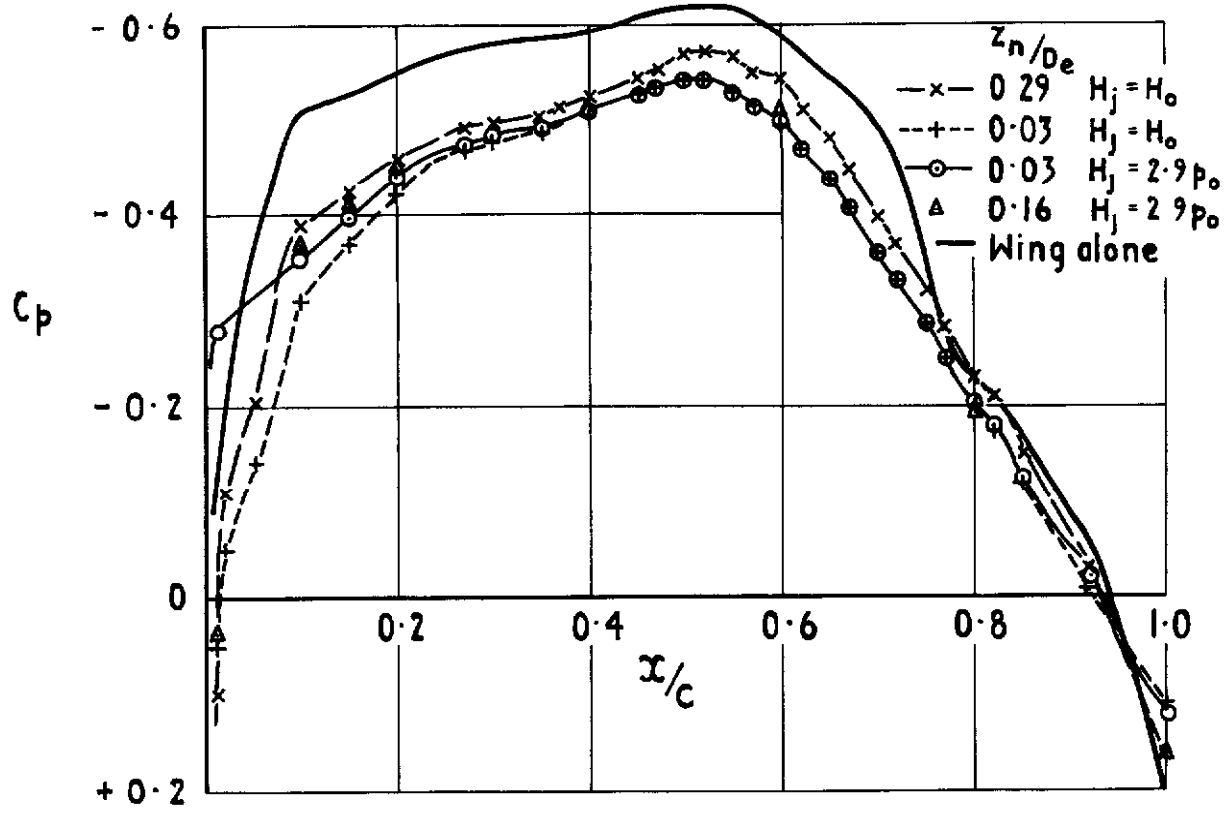

a $M_o = 0·72$

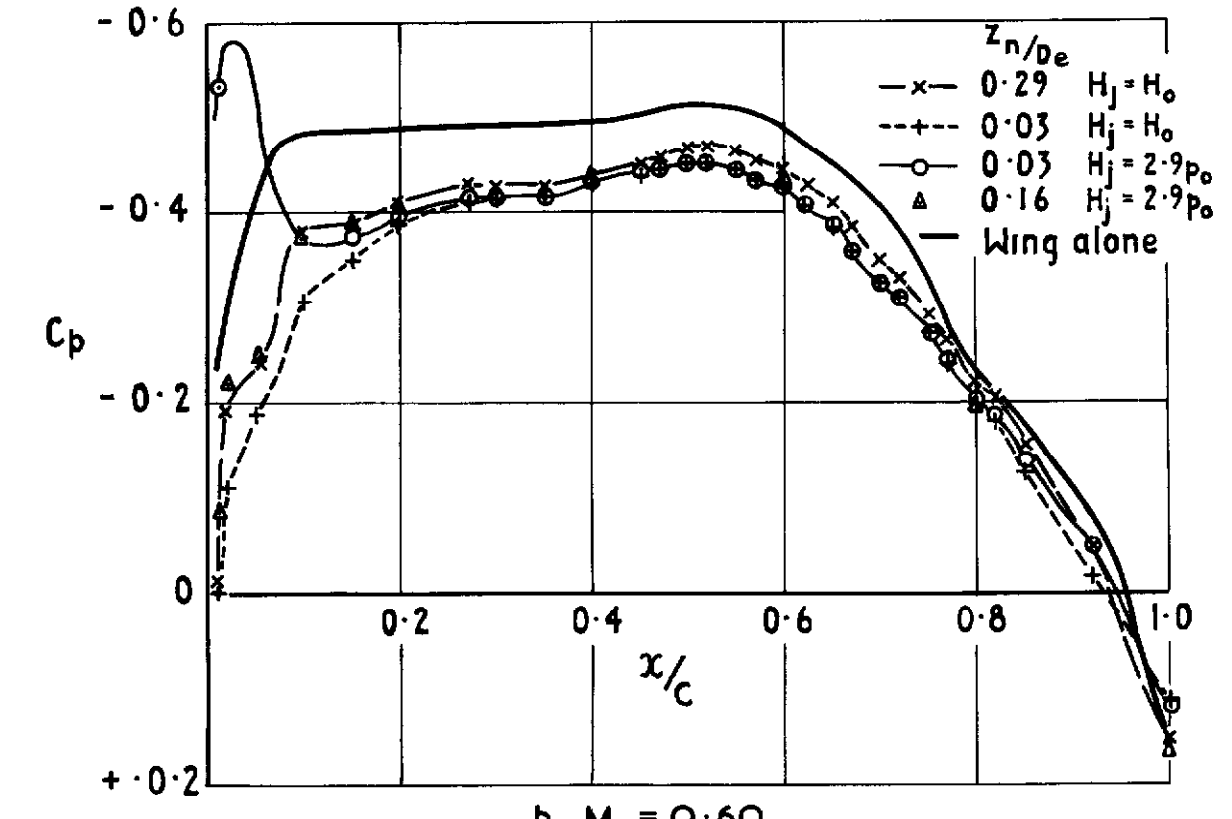

b $M_o = 0·60$

Fig.5 a & b Interference on the wing upper surface due to the jet pressure and position of the long nozzle $\alpha = 1·3^\circ$ $x_{n/De} = 0·38$

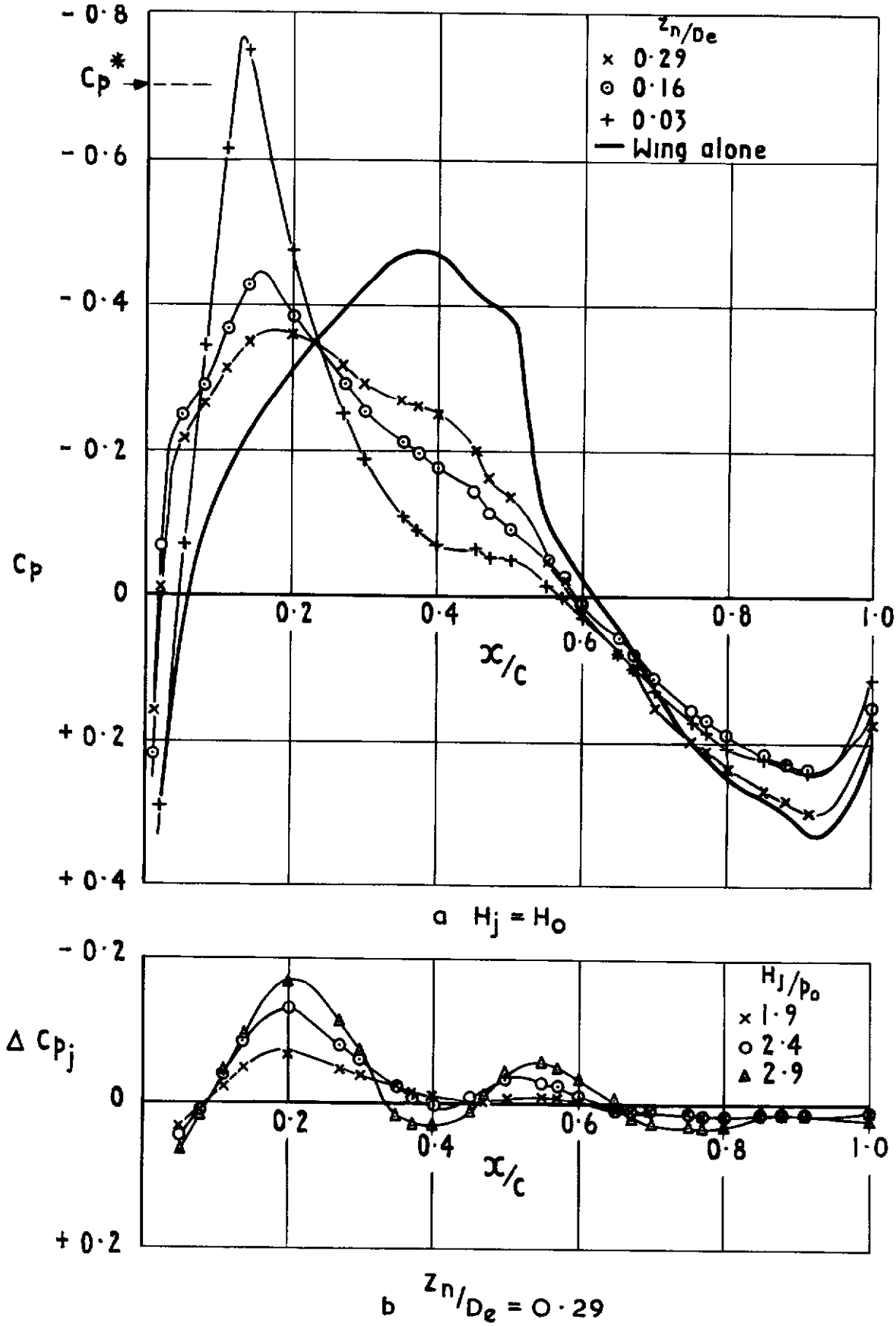

Fig. 6 a & b Interference on the wing lower surface with the long nozzle at three vertical positions. $M_o = 0 \cdot 72$, $\alpha = 1 \cdot 3^o$, $x_n/D_e = 0 \cdot 38$

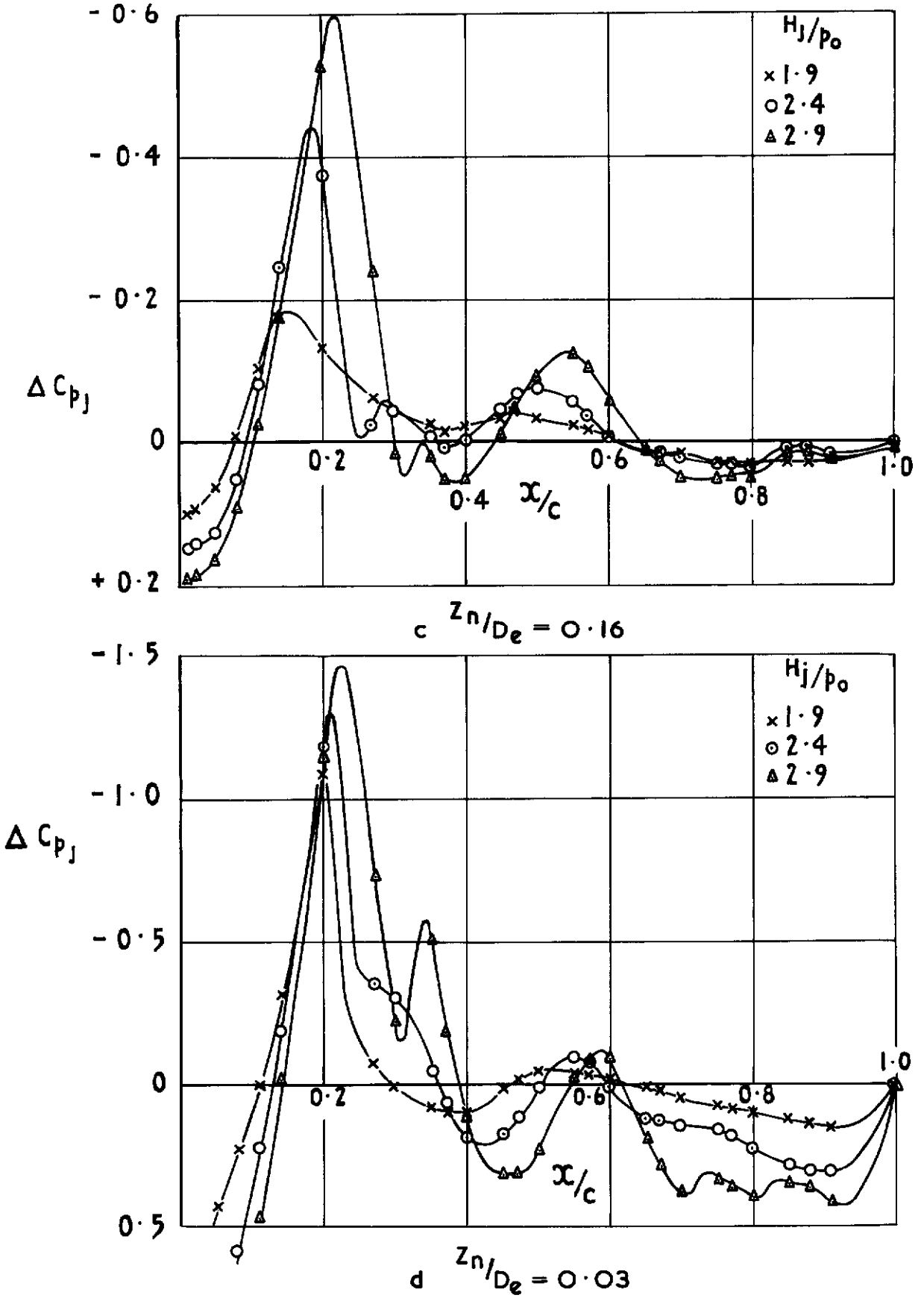

Fig. 6 c & d Interference on the wing lower surface with the long nozzle at three vertical positions. $M_0 = 0 \cdot 72$, $\alpha = 1 \cdot 3^\circ$ $x_n/D_e = 0 \cdot 38$

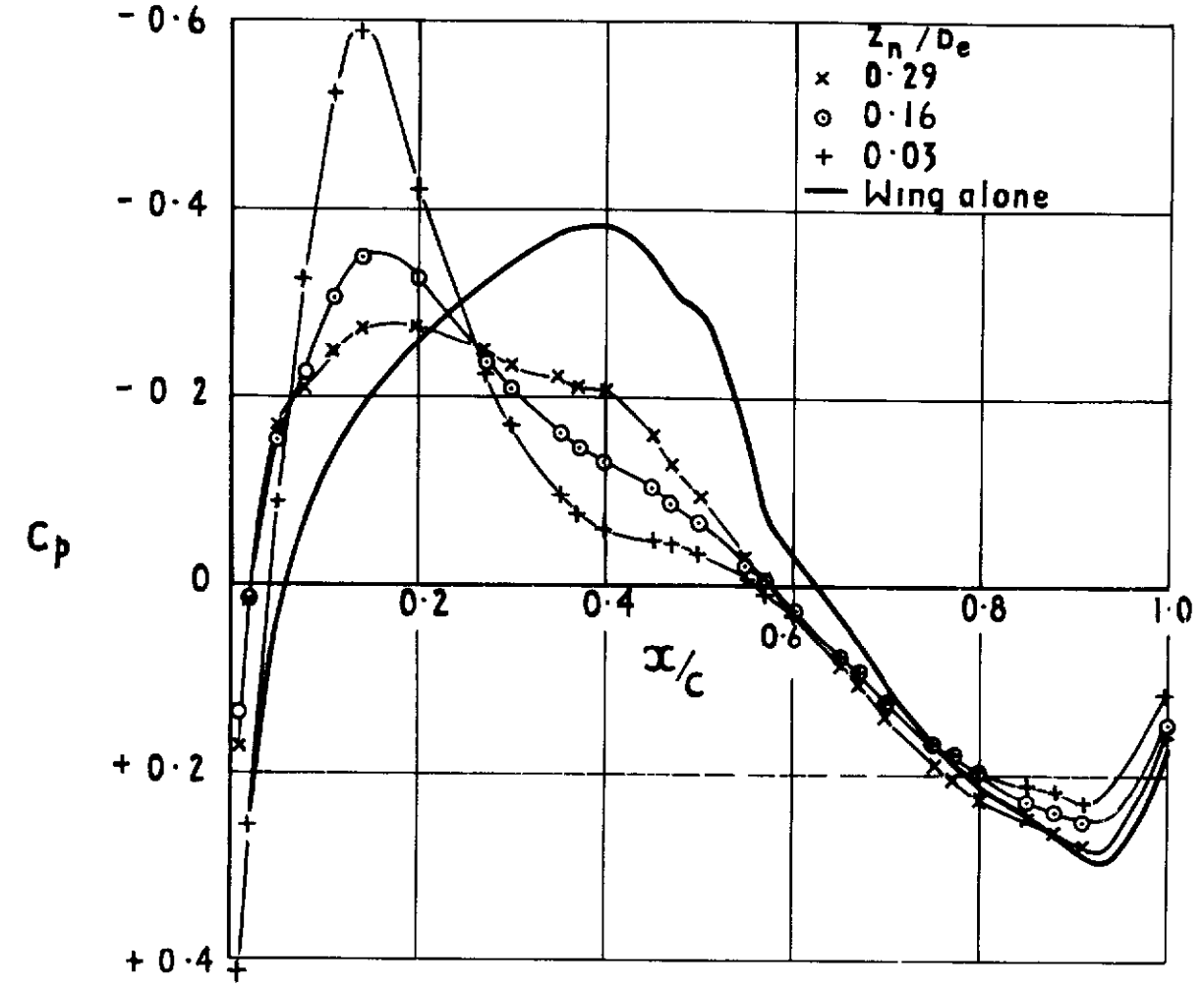

a $H_j = H_o$

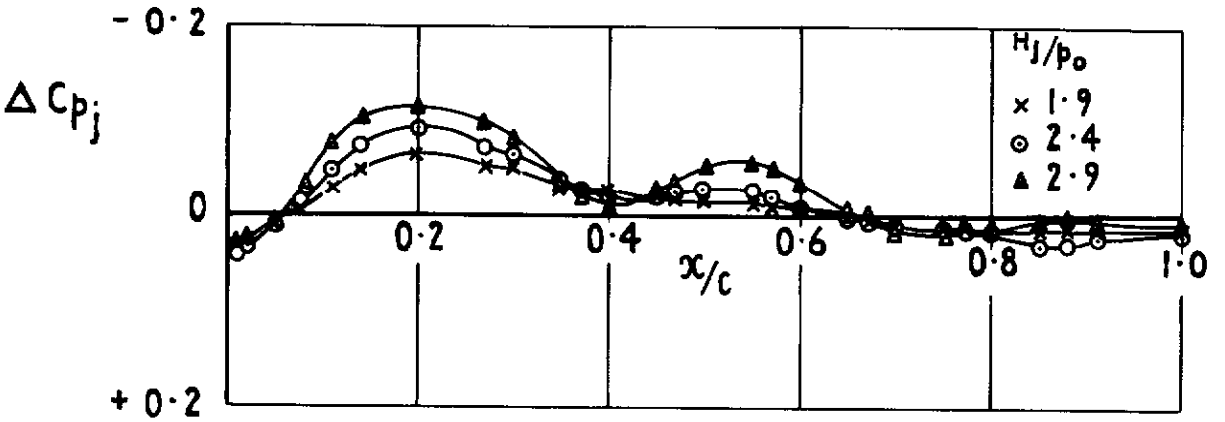

b $Z_n/D_e = 0 \cdot 29$

Fig.7 a & b Interference on the wing lower surface with the long nozzle at three vertical positions. $M_o = 0 \cdot 60$, $\alpha = 1 \cdot 3^o$, $x_n/D_e = 0 \cdot 38$

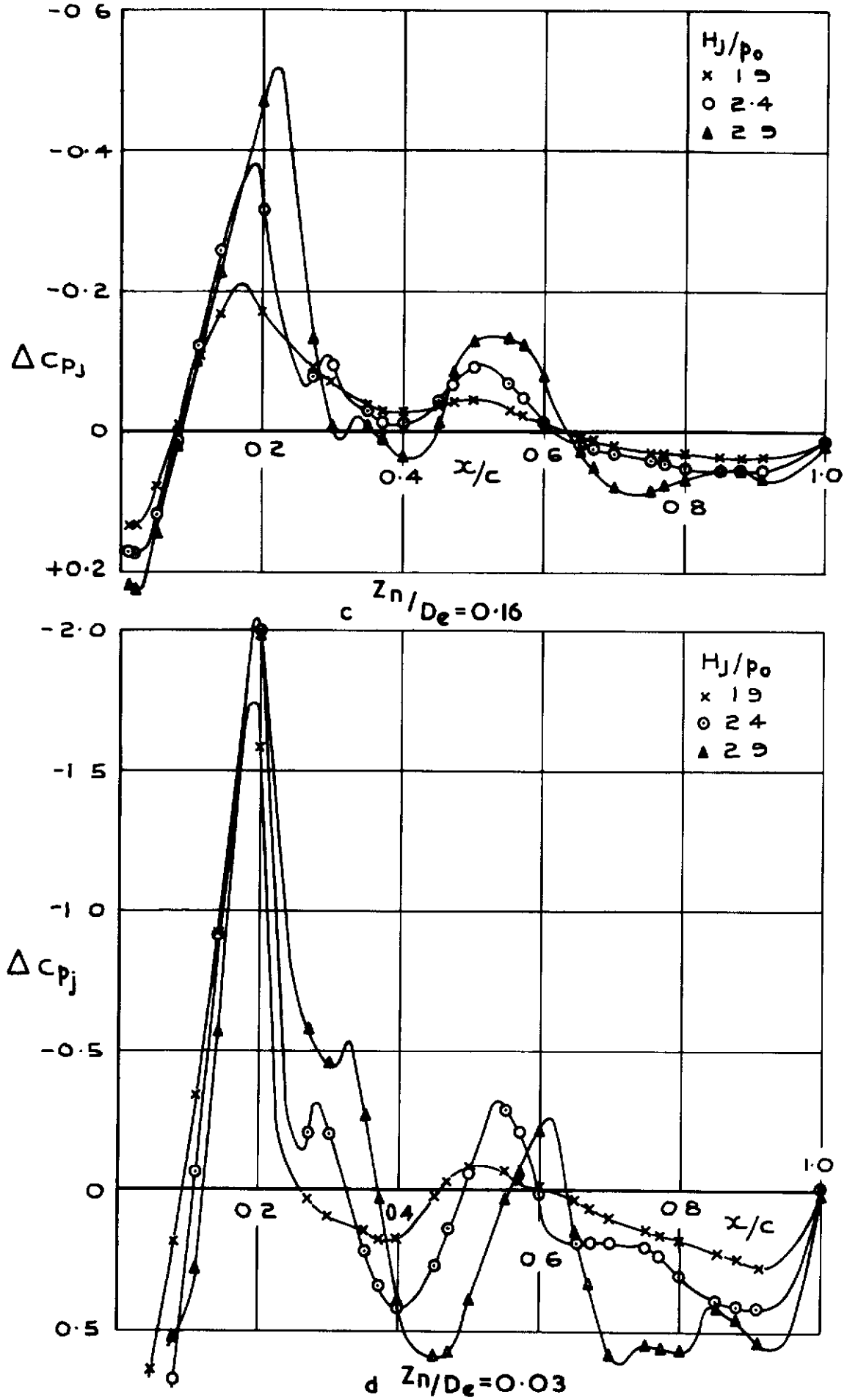

Fig.7 c & d Interference on the wing lower surface with the long nozzle at three vertical positions. $M_0 = 0{\cdot}60, \alpha = 1{\cdot}3^\circ$ $x_n/D_e = 0{\cdot}38$

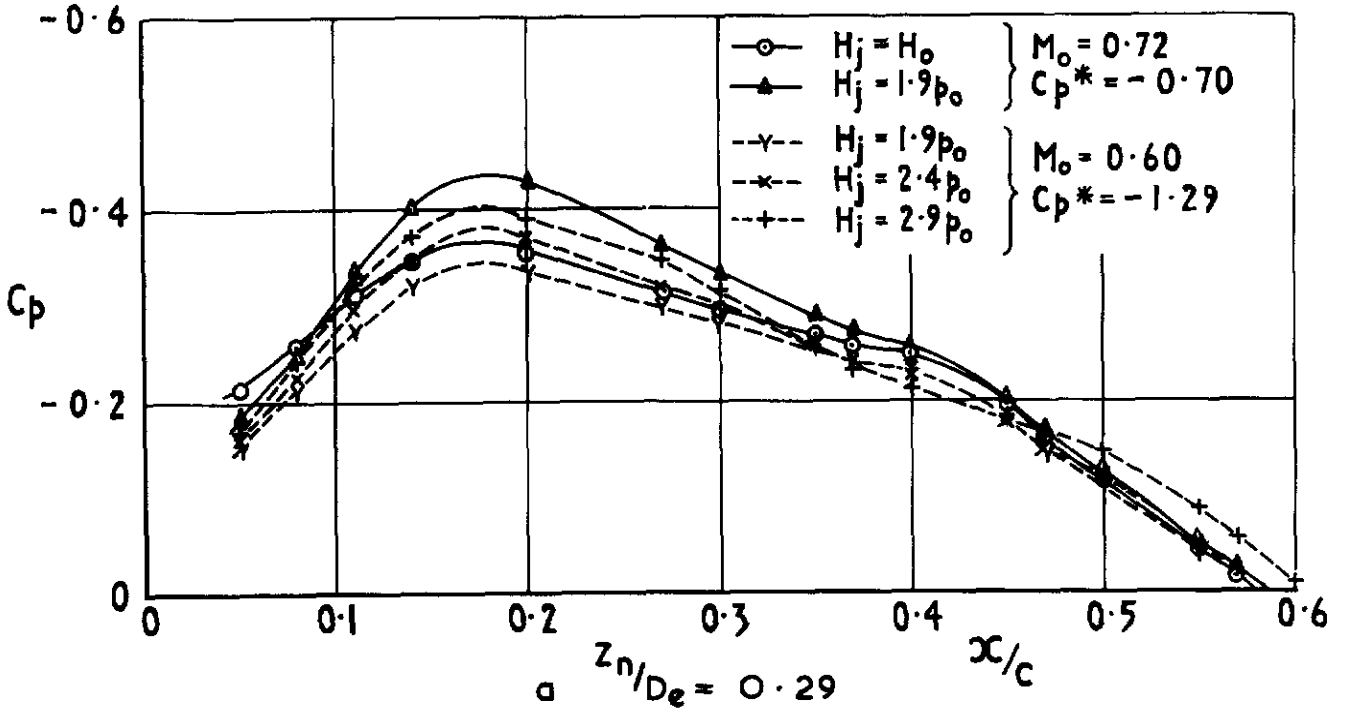

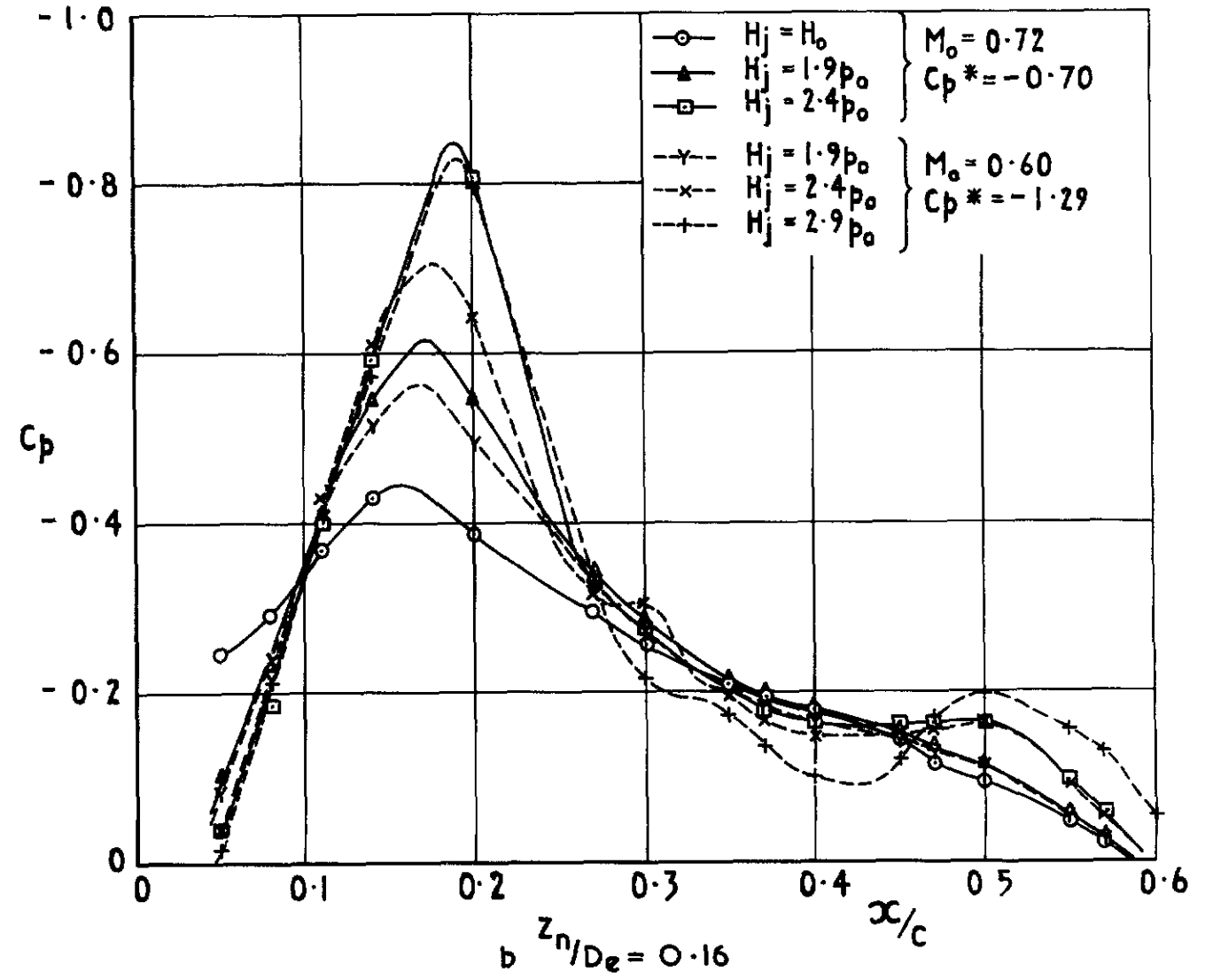

Fig.8 a & b Effect of Mach number on the pressure distribution on the wing lower surface. Long nozzle. $\alpha = 1 \cdot 3^{\circ}$ $x_n/D_e = 0 \cdot 38$

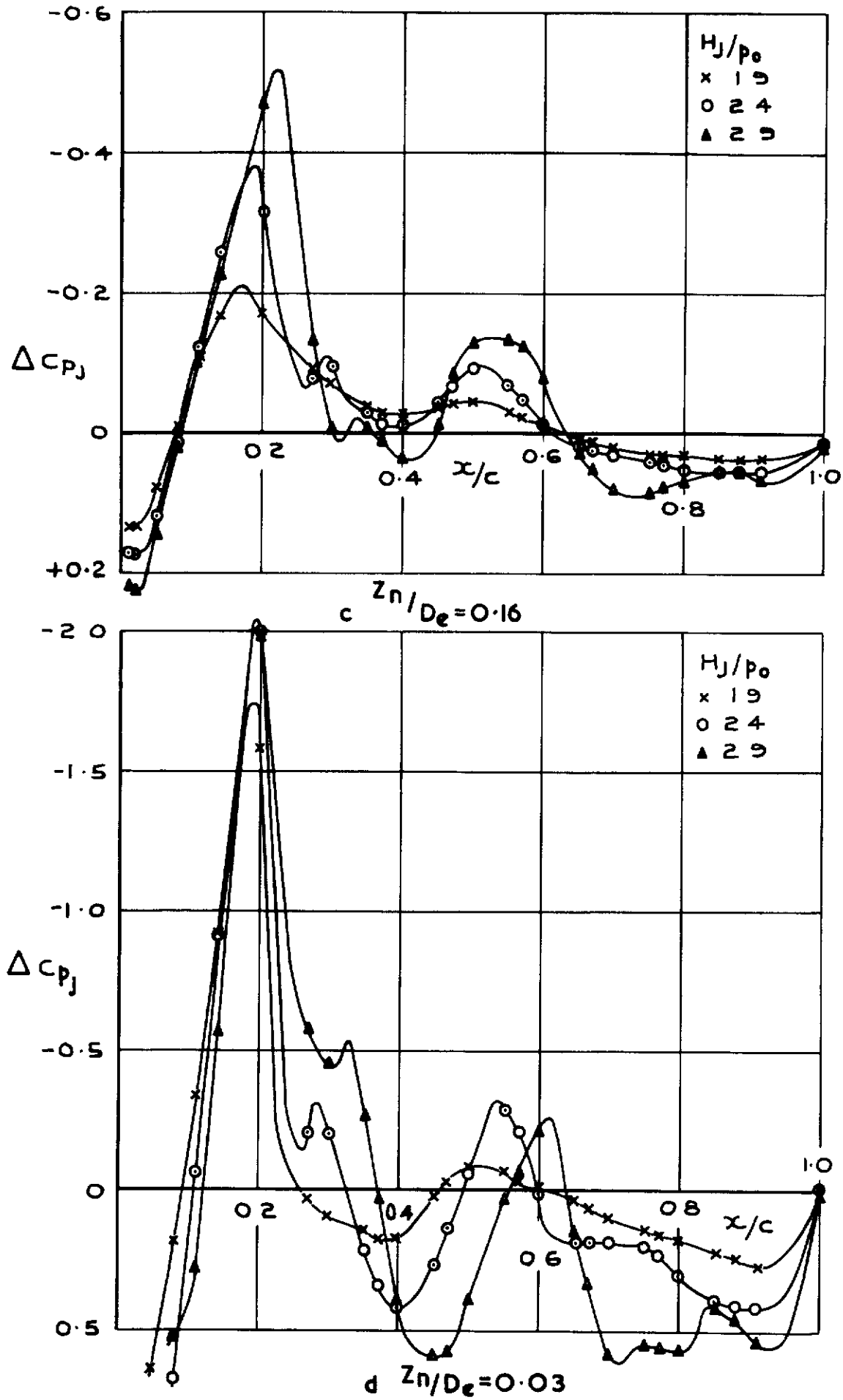

Fig.7 c & d Interference on the wing lower surface with the long nozzle at three vertical positions. $M_0 = 0{\cdot}60, \alpha = 1{\cdot}3^\circ$ $x_n/D_e = 0{\cdot}38$

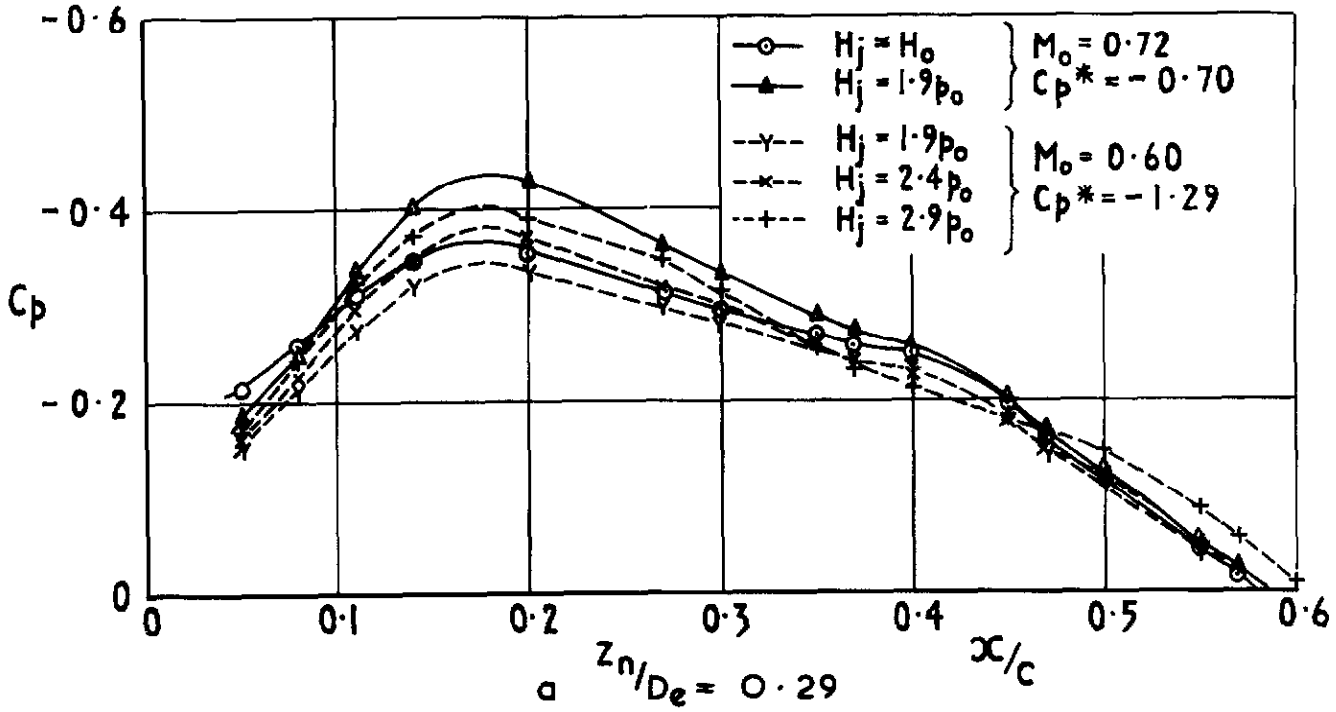

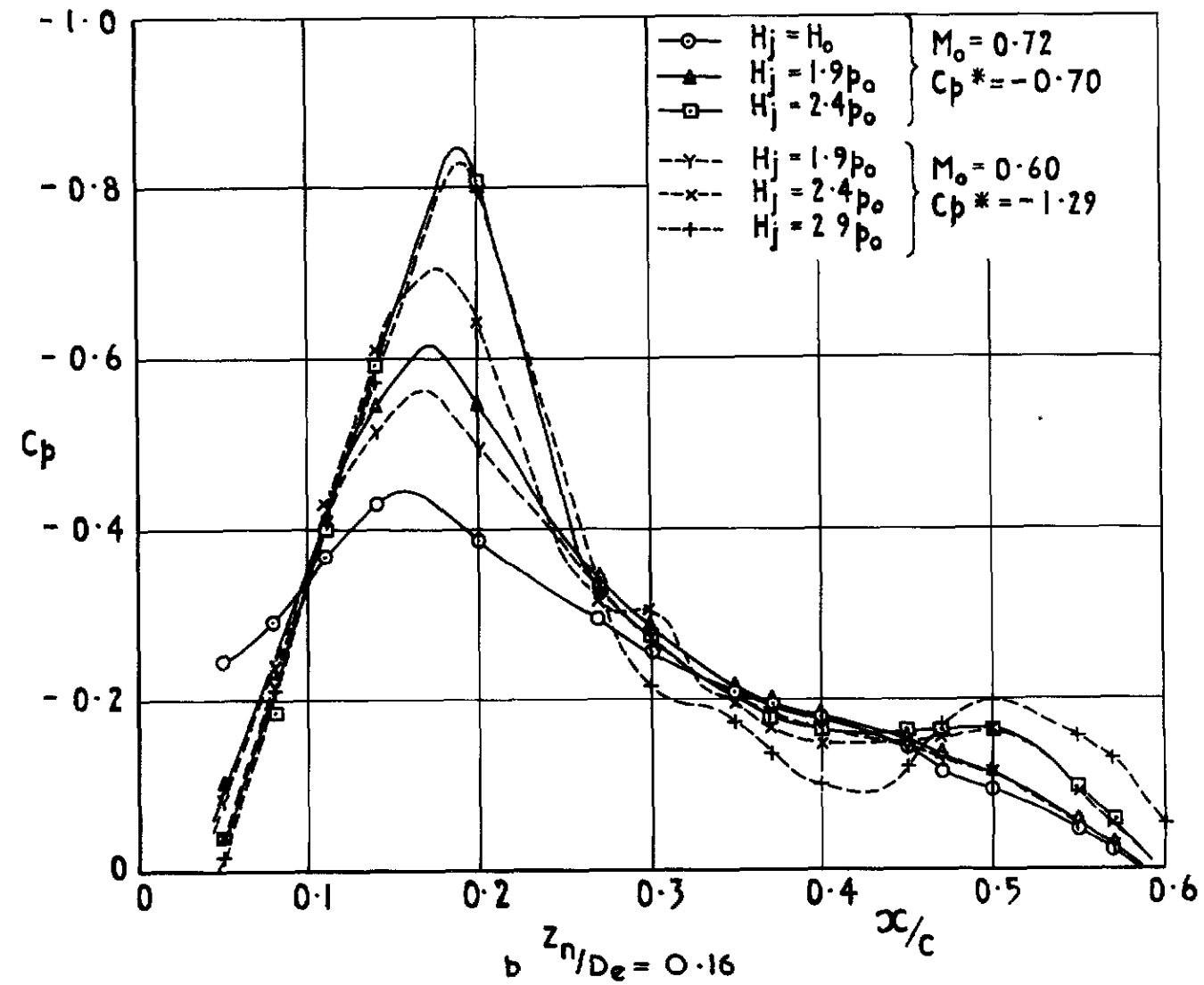

Fig.8 a & b Effect of Mach number on the pressure distribution on the wing lower surface. Long nozzle. $\alpha = 1 \cdot 3^{\circ}$ $x_n/D_e = 0 \cdot 38$

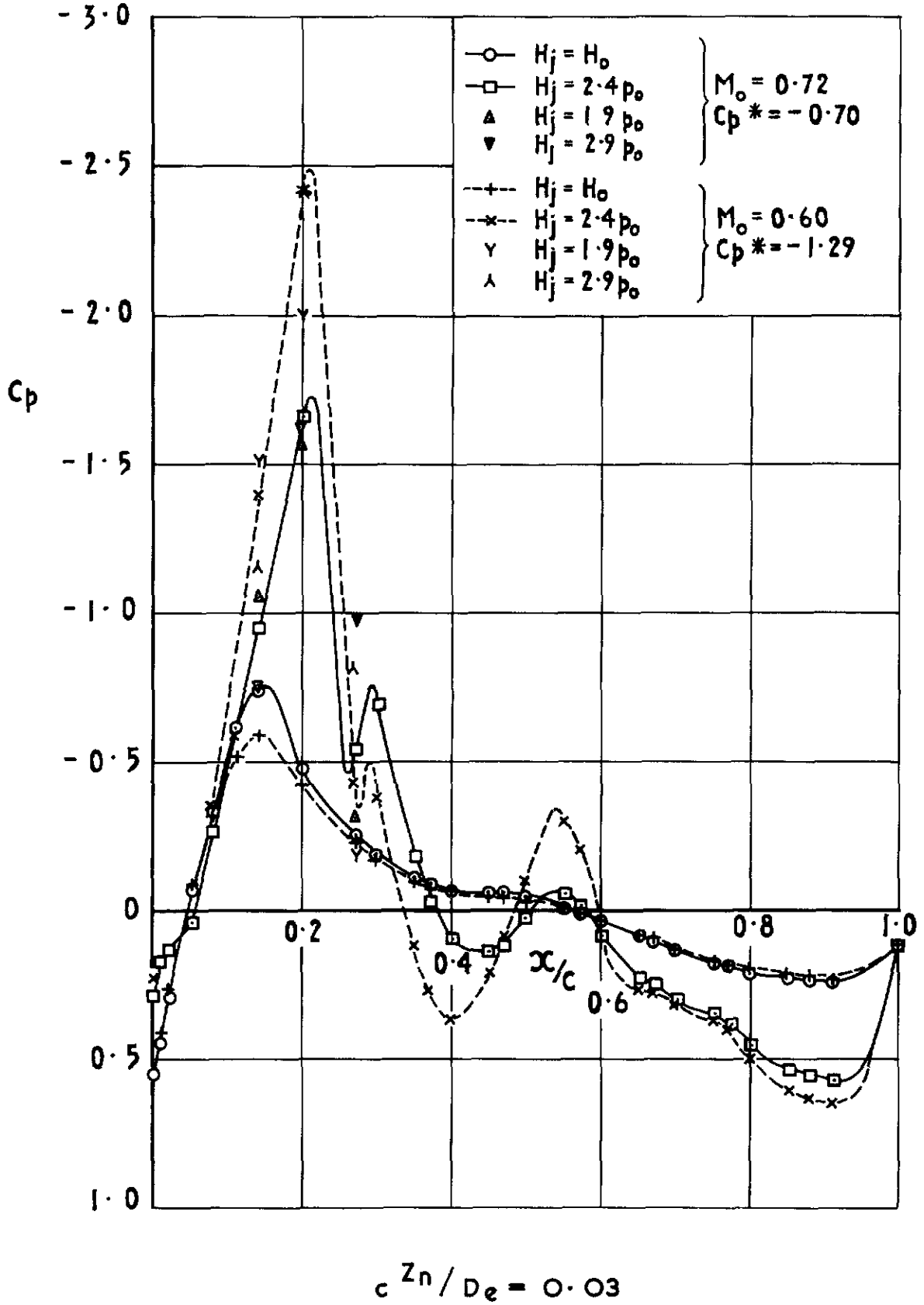

Fig 8 c Effect of Mach number on the pressure distribution on the wing lower surface. Long nozzle. $\alpha = 1·3°$, $^{x_n}/_{D_e} = 0\ 38$

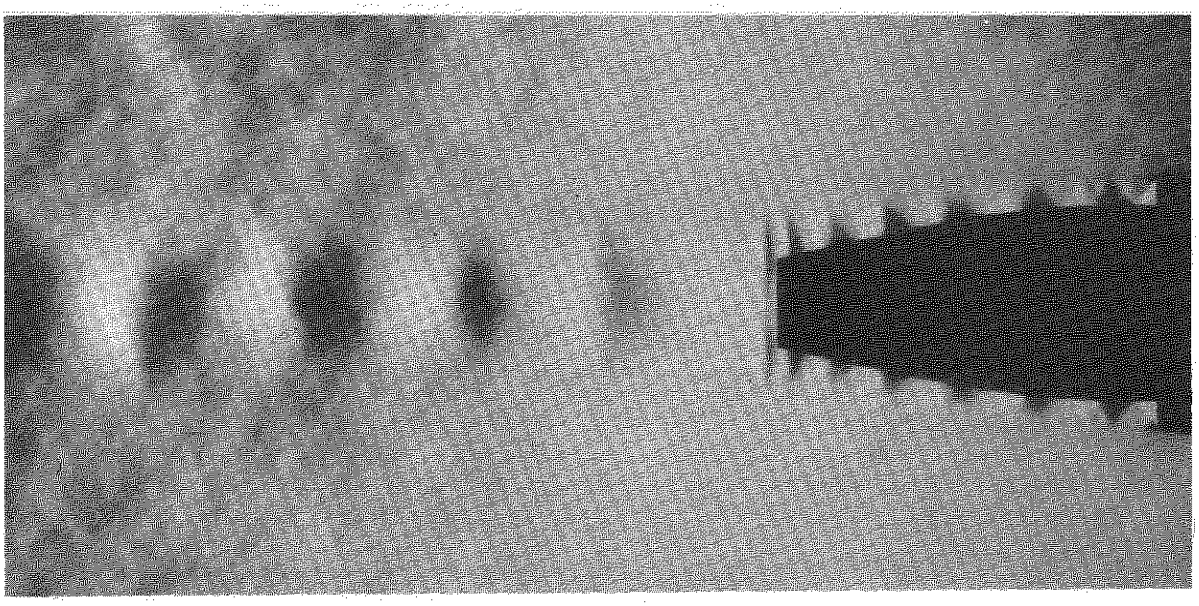

a $M_o = 0.7$ $H_j/p_o = 2.4$

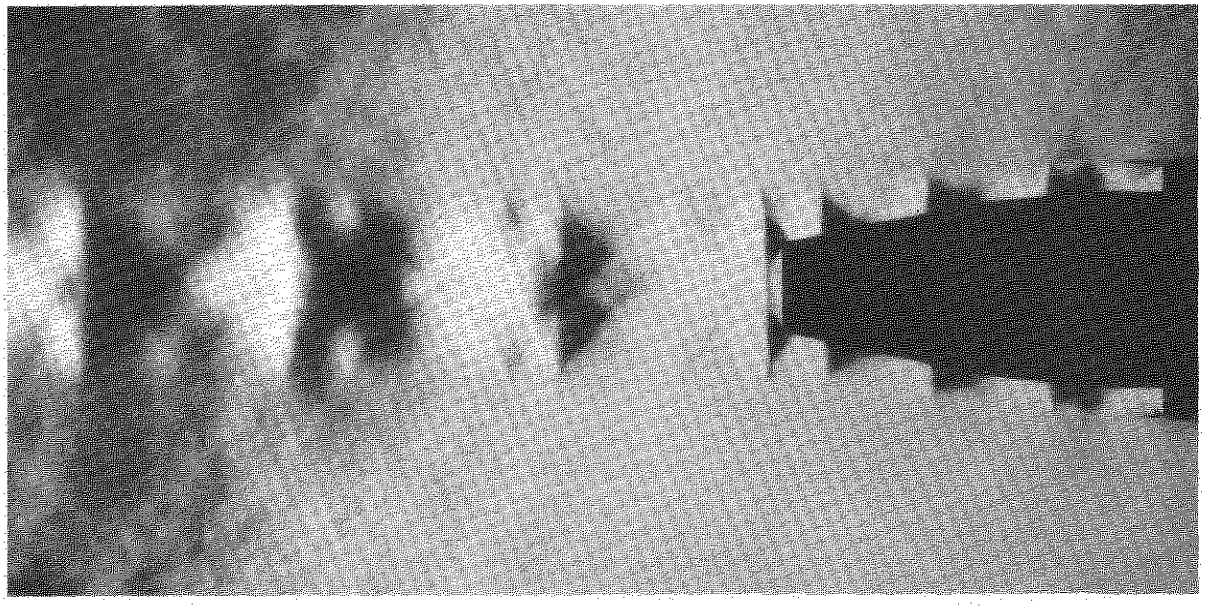

b $M_o = 0.7$ $H_j/p_o = 3.0$

Fig.9 Schlieren photographs of flow from bypass nozzle

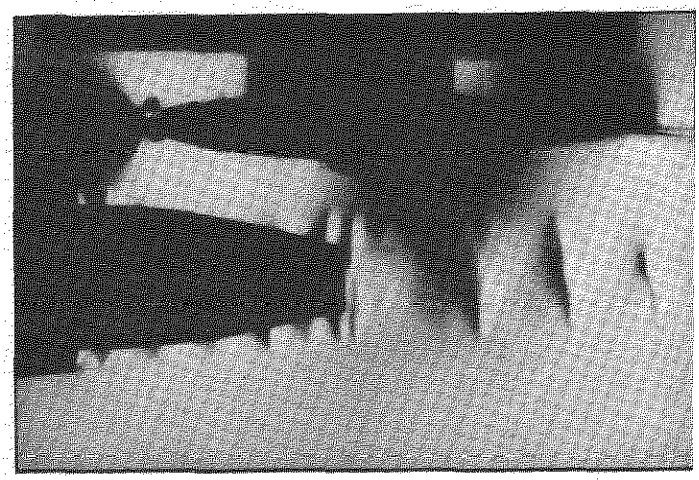

$M_o = 0{\cdot}72$: $H_j/p_o = 2{\cdot}4$: $z_n/D_e = 0{\cdot}29$

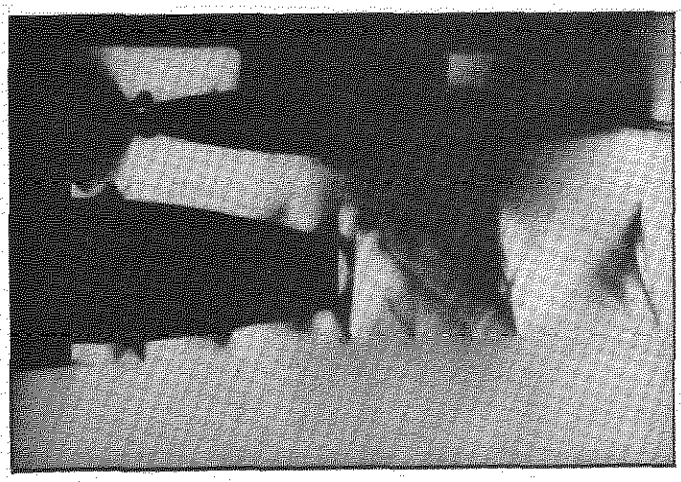

$M_o = 0{\cdot}72$: $H_j/p_o = 2{\cdot}9$: $z_n/D_e = 0{\cdot}29$

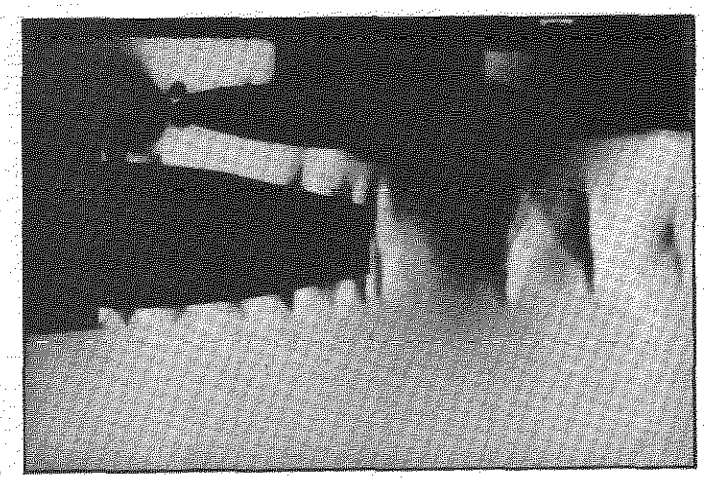

$M_o = 0{\cdot}72$: $H_j/p_o = 2{\cdot}4$: $z_n/D_e = 0{\cdot}16$

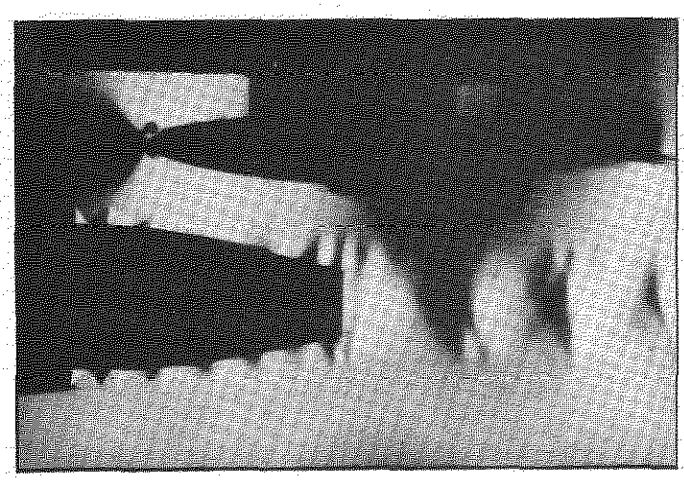

$M_o = 0{\cdot}60$: $H_j/p_o = 2{\cdot}4$: $z_n/D_e = 0{\cdot}29$

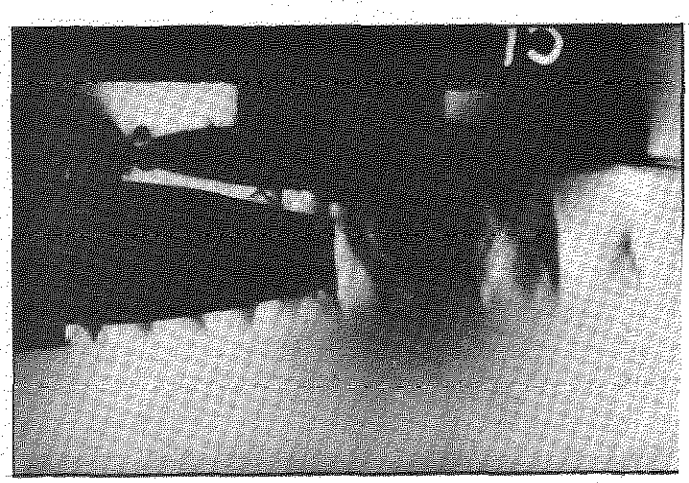

$M_o = 0{\cdot}72$: $H_j/p_o = 2{\cdot}4$: $z_n/D_e = 0{\cdot}03$

Fig.10 Schlieren studies with the long nozzle

$\alpha = 1{\cdot}3°$: $x_n/D_e = 0{\cdot}38$

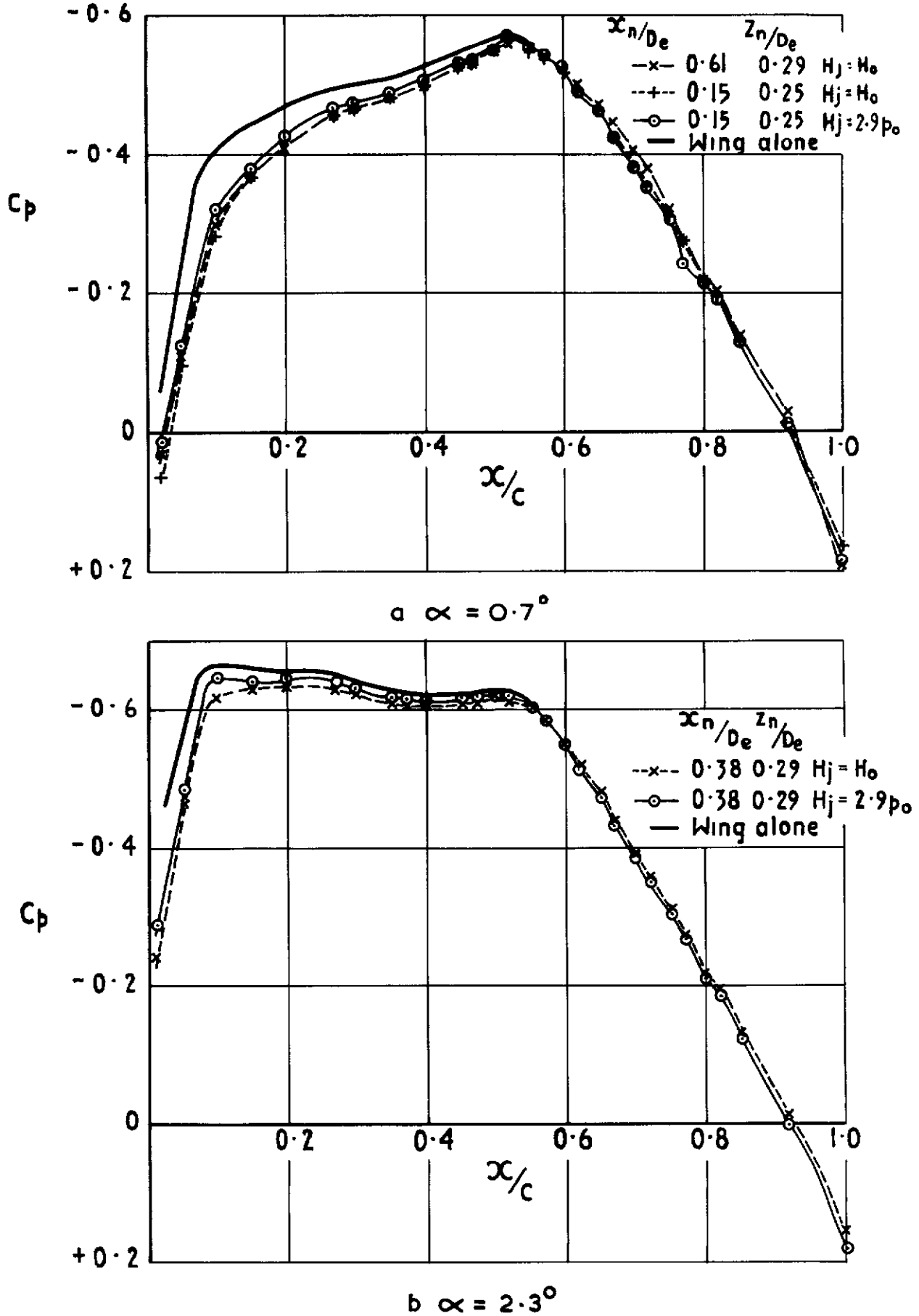

Fig.11 a & b Interference on the wing upper surface due to the jet pressure and position of the short nozzle. $M_o = 0{\cdot}72$

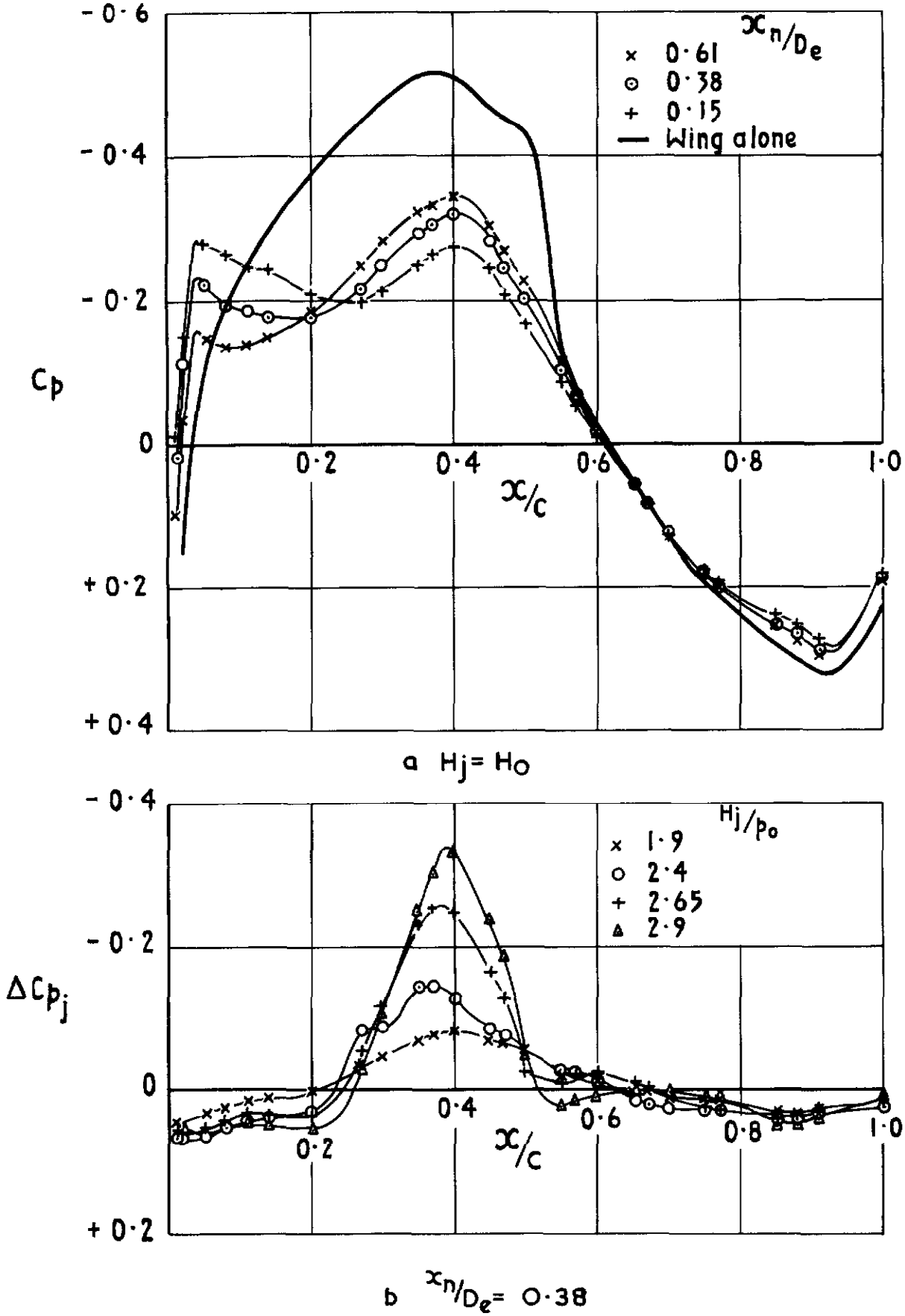

Fig. 12 a & b Interference on the wing lower surface with the short nozzle at three horizontal positions. $Z_n/D_e = 0·29$, $M_o = 0·72$, $\alpha = 0·7°$

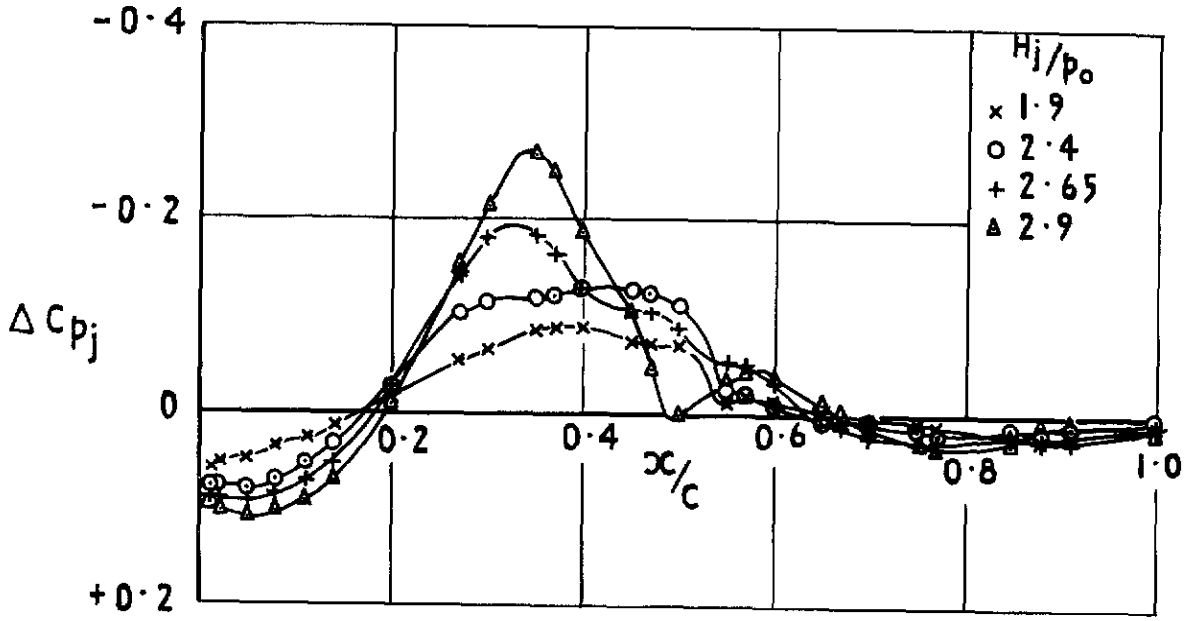

c $x_n/D_e = 0 \cdot 61$

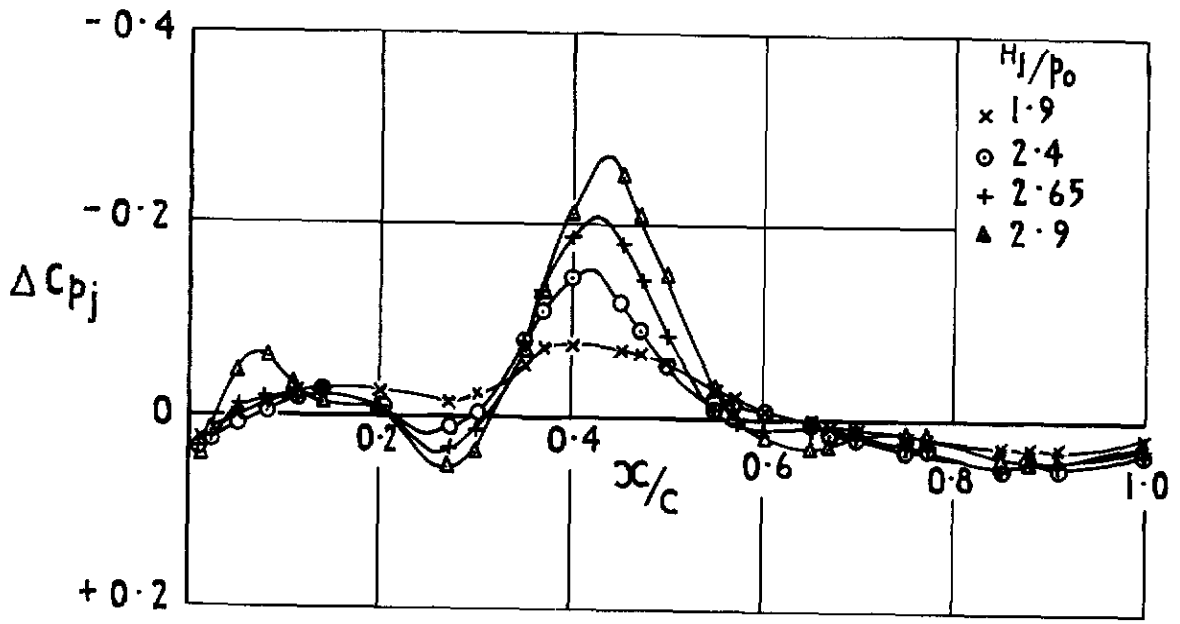

d $x_n/D_e = 0 \cdot 15$

Fig 12 c & d Interference on the wing lower surface with the short nozzle at three horizontal positions. $Z_n/D_e = 0 \cdot 29$, $M_0 = 0 \cdot 72$, $\alpha = 0 \cdot 7°$

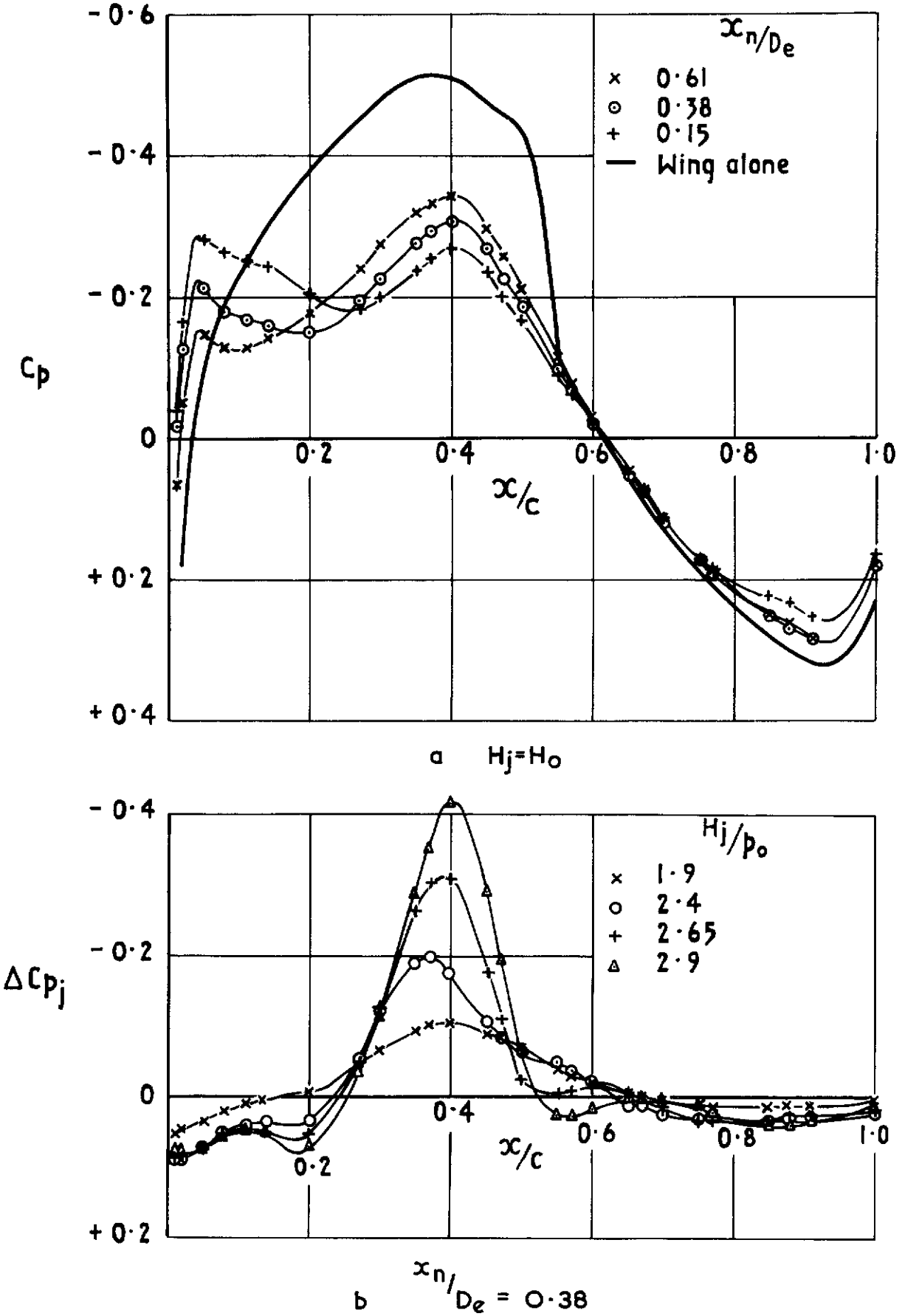

Fig 13 a & b Interference on the wing lower surface with the short nozzle at three horizontal positions. $Z_{n/D_e} = 0·25$, $M_o = 0·72$, $\alpha = 0·7°$

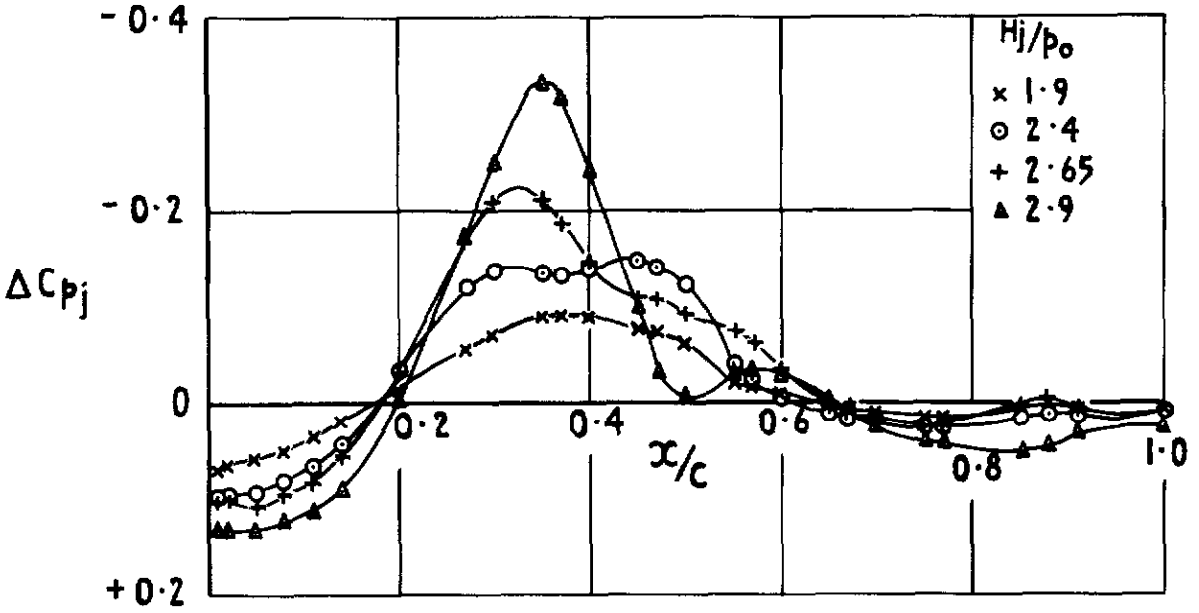

c $x_n/D_e = 0 \cdot 61$

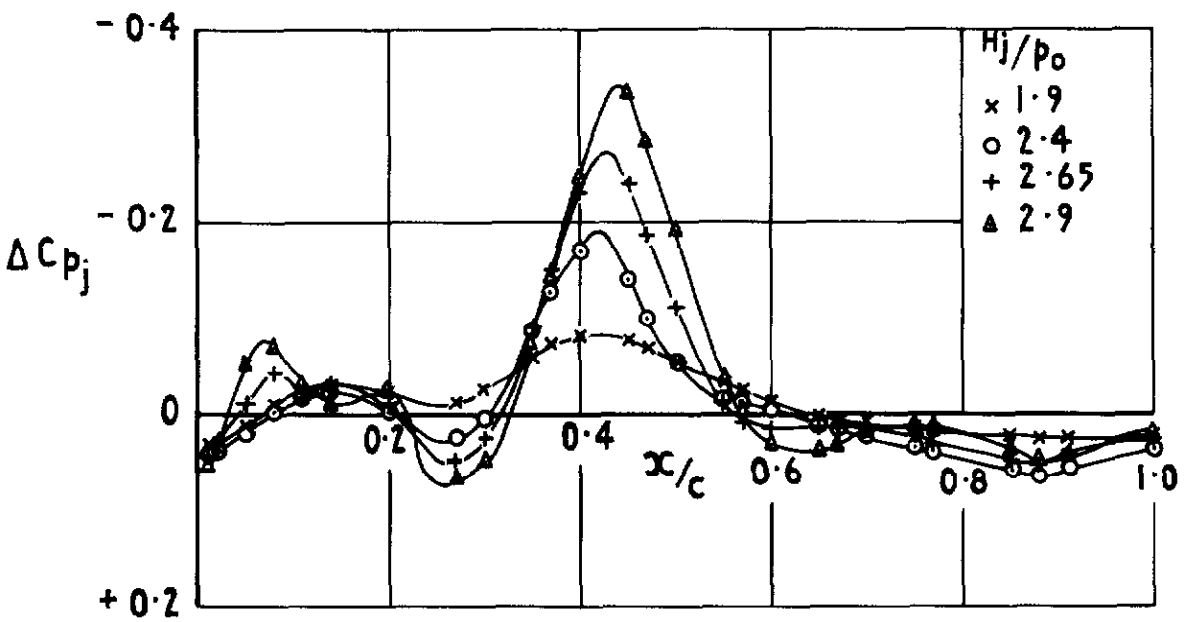

d $x_n/D_e = 0 \cdot 15$

Fig. 13 c & d Interference on the wing lower surface with the short nozzle at three horizontal positions. $Z_n/D_e = 0 \cdot 25$, $M_o = 0 \cdot 72$, $\alpha = 0 \cdot 7°$

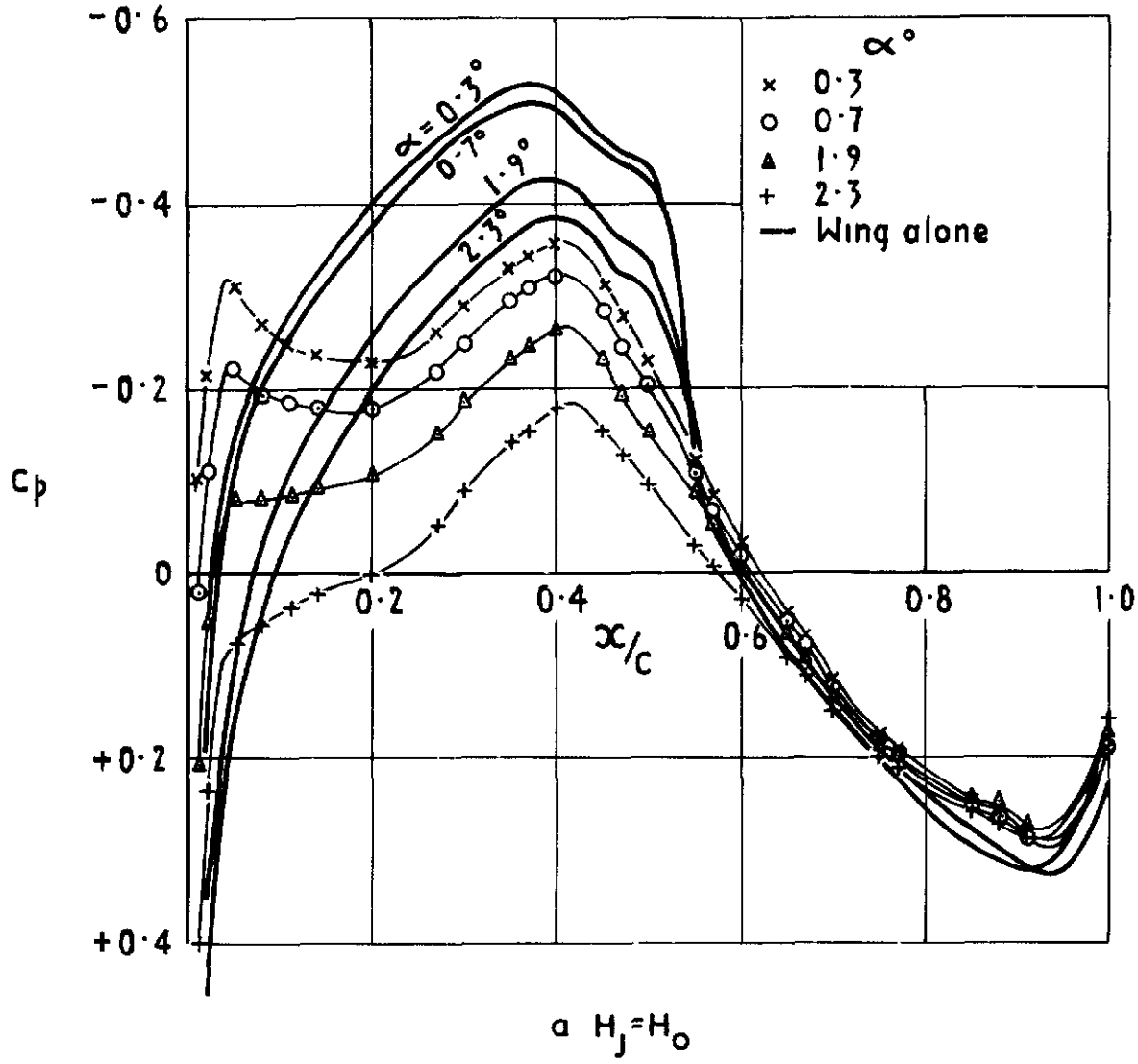

Fig 14 a The effect of wing incidence and jet interference on the wing lower surface. With the short nozzle at $x_n/D_e = 0{\cdot}38$, $Z_n/D_e = 0{\cdot}29$. $M_o = 0{\cdot}72$

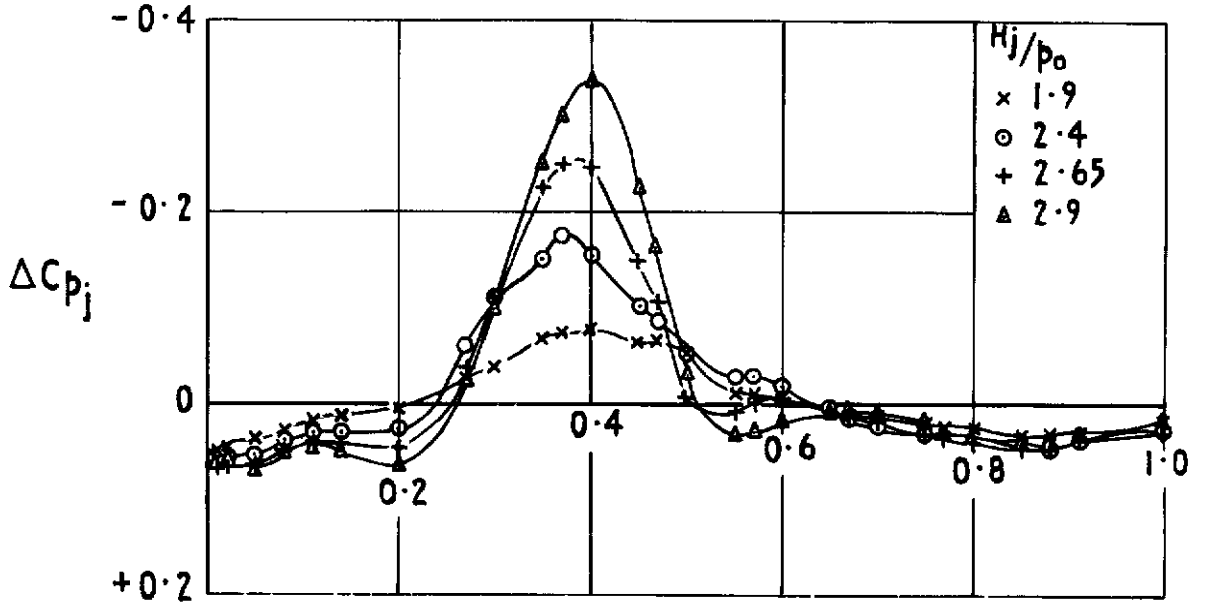

b α=0 3°

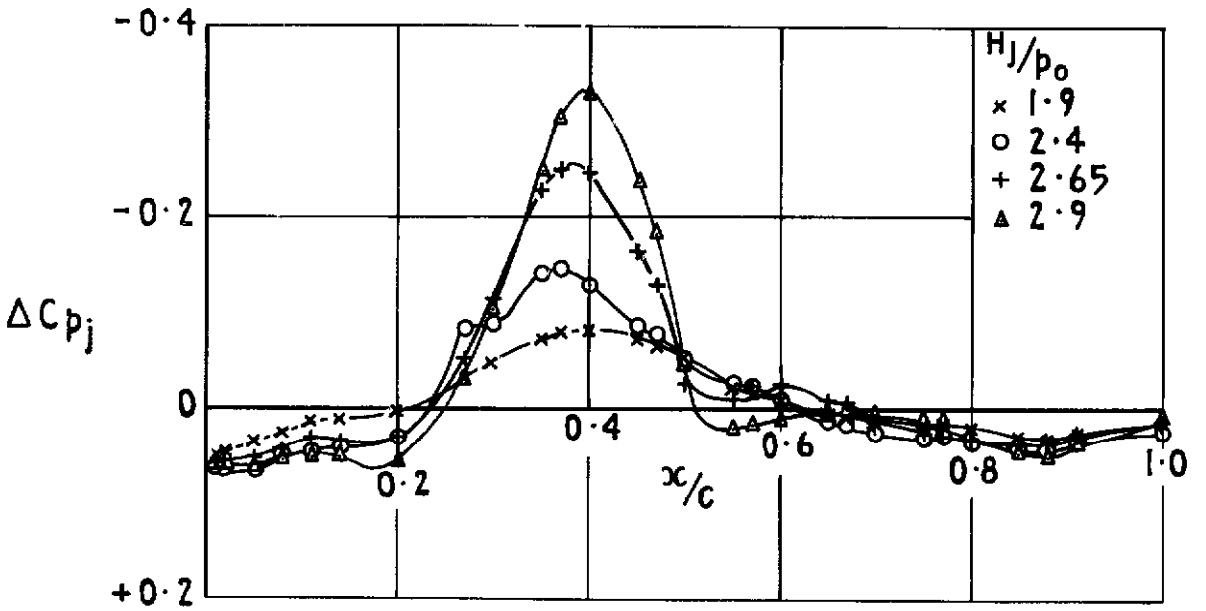

c α=0·7°

Fig. 14 b & c The effect of wing incidence and jet interference on the wing lower surface. With the short nozzle at x_n/D_e = 0·38, Z_n/D_e = 0·29. M_0 = 0·72

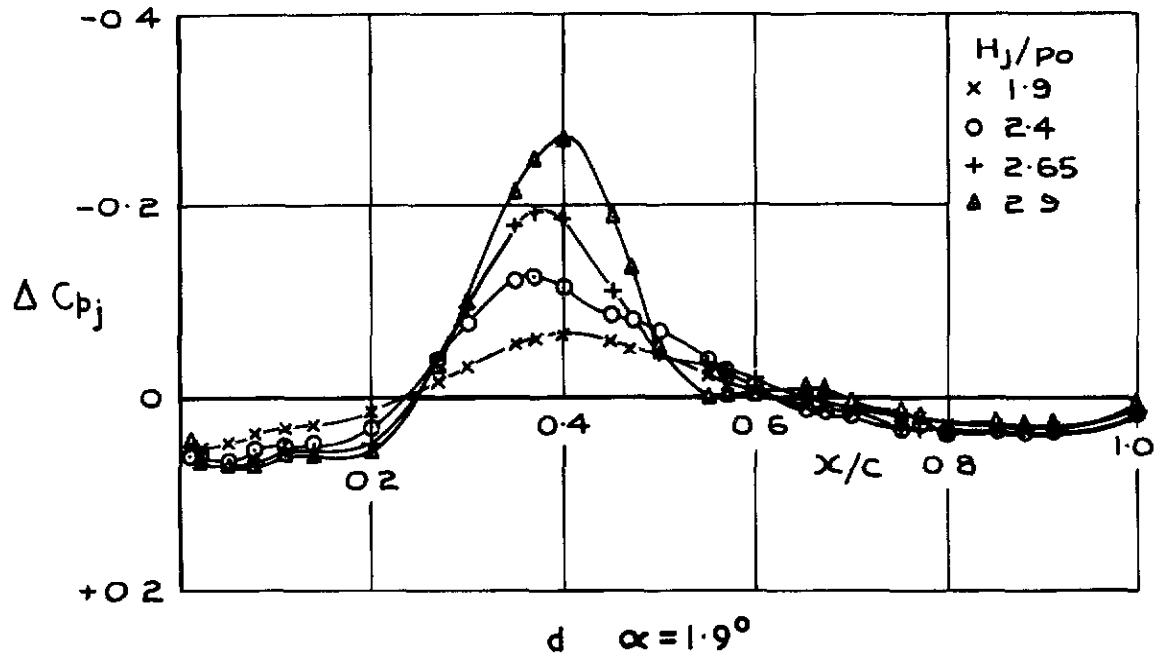

d $\alpha = 1{\cdot}9^{\circ}$

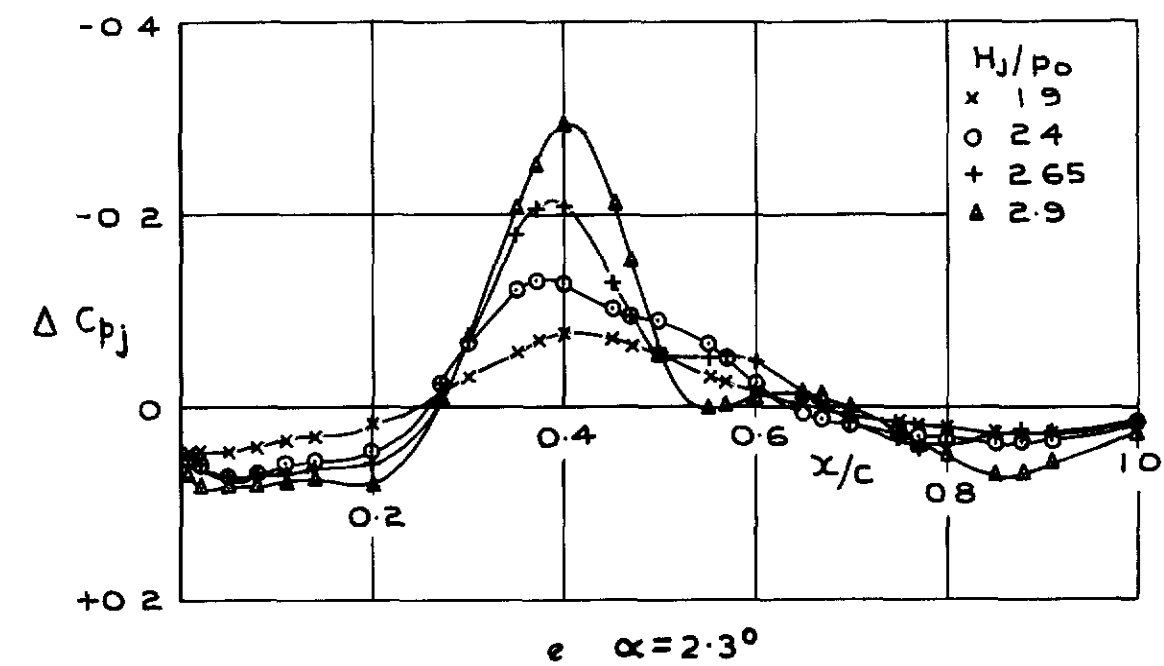

e $\alpha = 2{\cdot}3^{\circ}$

Fig. 14 d & e The effect of wing incidence and jet interference on the wing lower surface. With the short nozzle at $^{x_n}/_{D_e} = 0{\cdot}38$, $^{z_n}/_{D_e} = 0{\cdot}29$. $M_o = 0{\cdot}72$

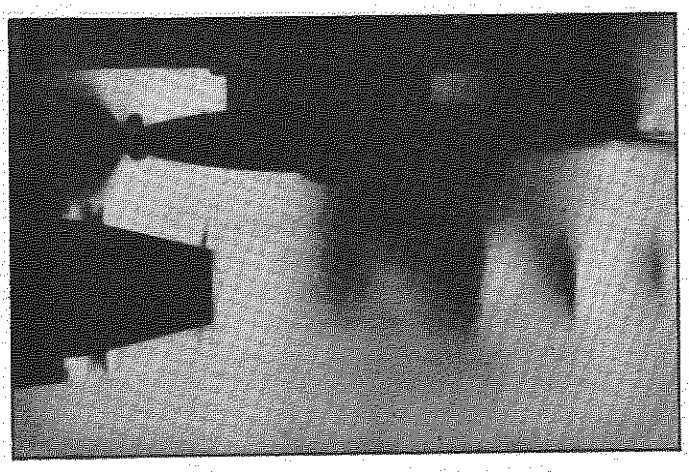

$\alpha = 0{\cdot}7°$: $H_j/p_o = 2{\cdot}4$

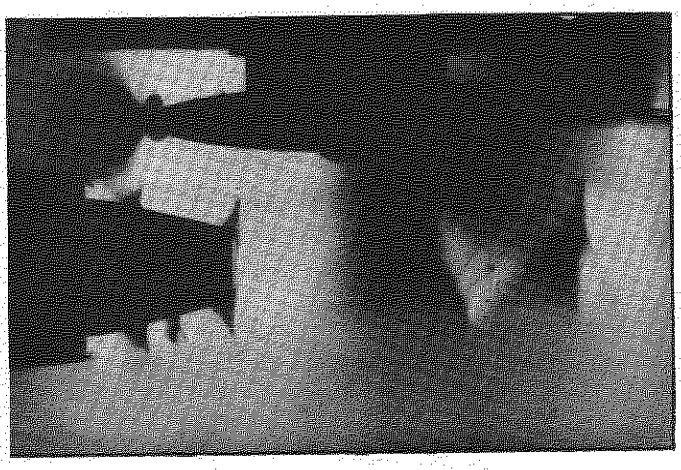

$\alpha = 0{\cdot}7°$: $H_j/p_o = 2{\cdot}9$

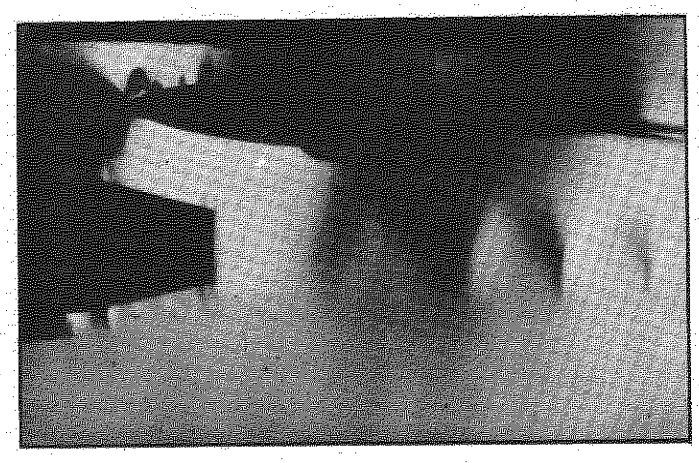

Schlieren knife-edge vertical

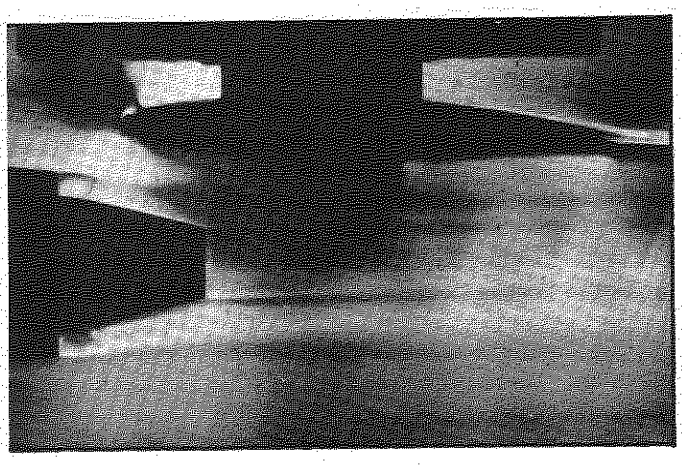

Schlieren knife-edge horizontal

$\alpha = 2{\cdot}3°$: $H_j/p_o = 2{\cdot}4$

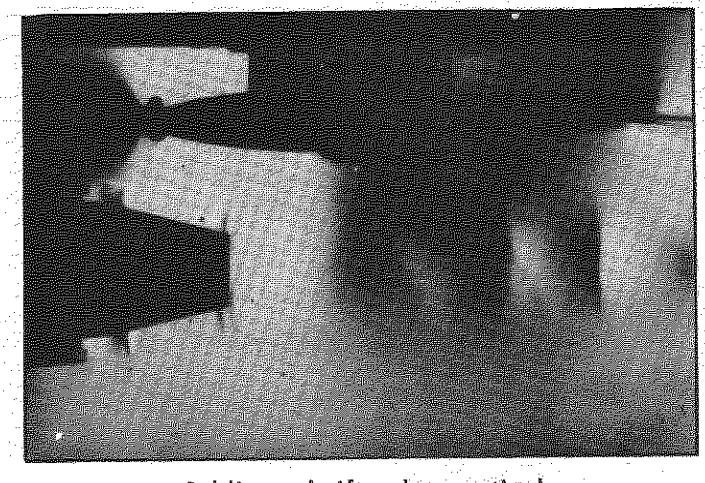

Schlieren knife-edge vertical

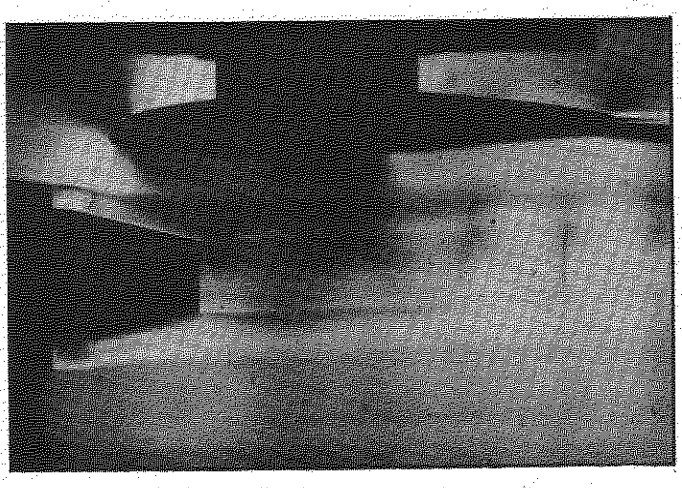

Schlieren knife-edge horizontal

$\alpha = 0{\cdot}3°$: $H_j/p_o = 2{\cdot}4$

Fig.15 Schlieren studies with the short nozzle

$M_o = 0{\cdot}72$: $x_n/D_e = 0{\cdot}38$: $z_n/D_e = 0{\cdot}29$

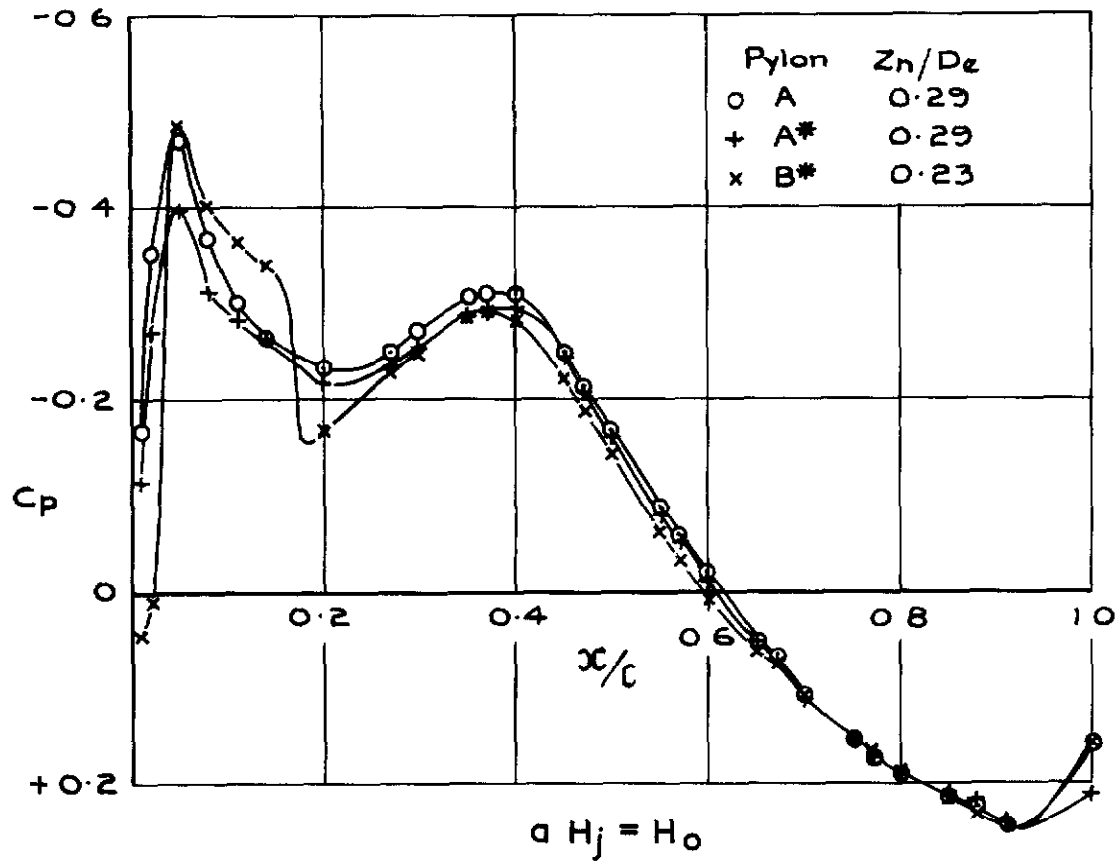

a $H_j = H_o$

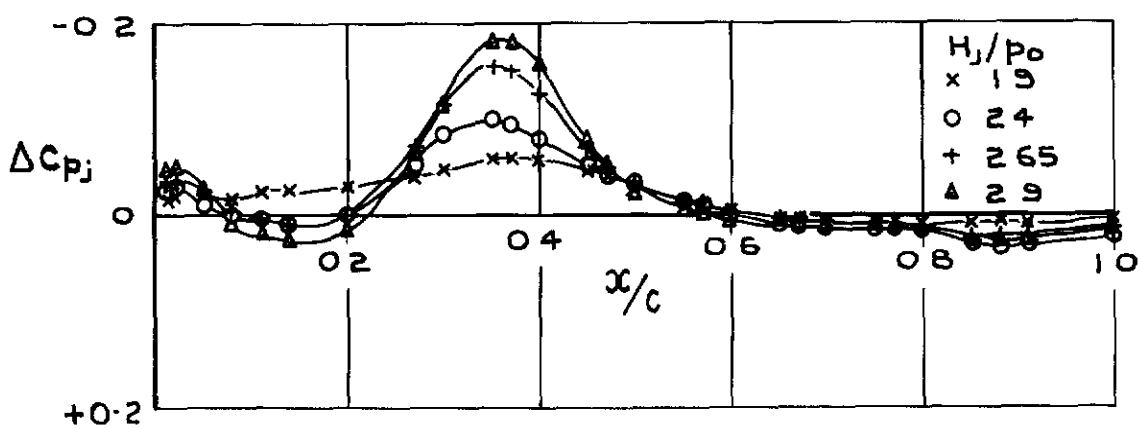

b Pylon A · $Z_n/D_e = 0.29$

Fig. 16 a & b The effect of three pylons with jet interference on the wing lower surface. With the short nozzle at $x_n/D_e = 0.38$. $M_o = 0.72$ and $\alpha = 0\,5^\circ$

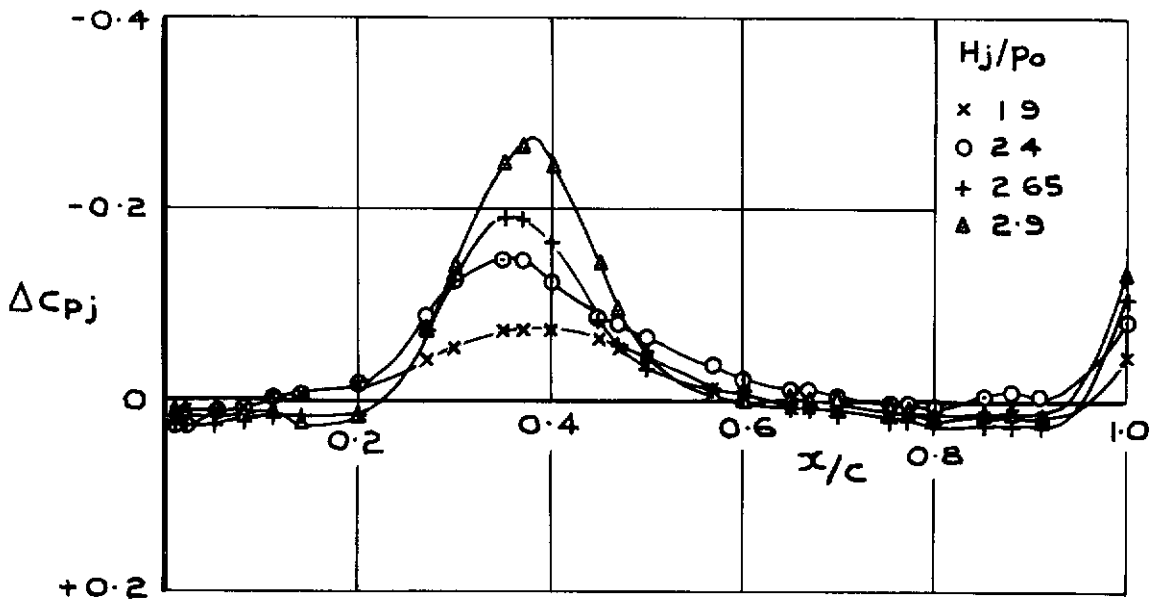

c Pylon A*: $Z_n/D_e = 0.29$

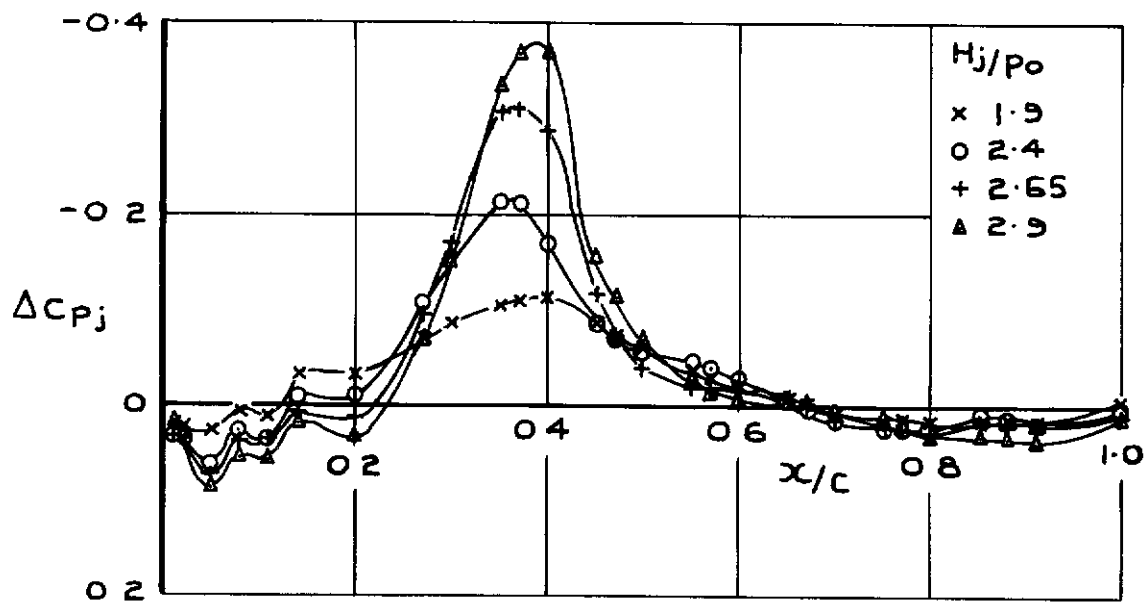

d Pylon B*: $Z_n/D_e = 0.23$

Fig. 16 c & d The effect of three pylons with jet interference on the wing lower surface. With the short nozzle at $x_n/D_e = 0.38$. $M_o = 0.72$ and $\alpha = 0.5^\circ$

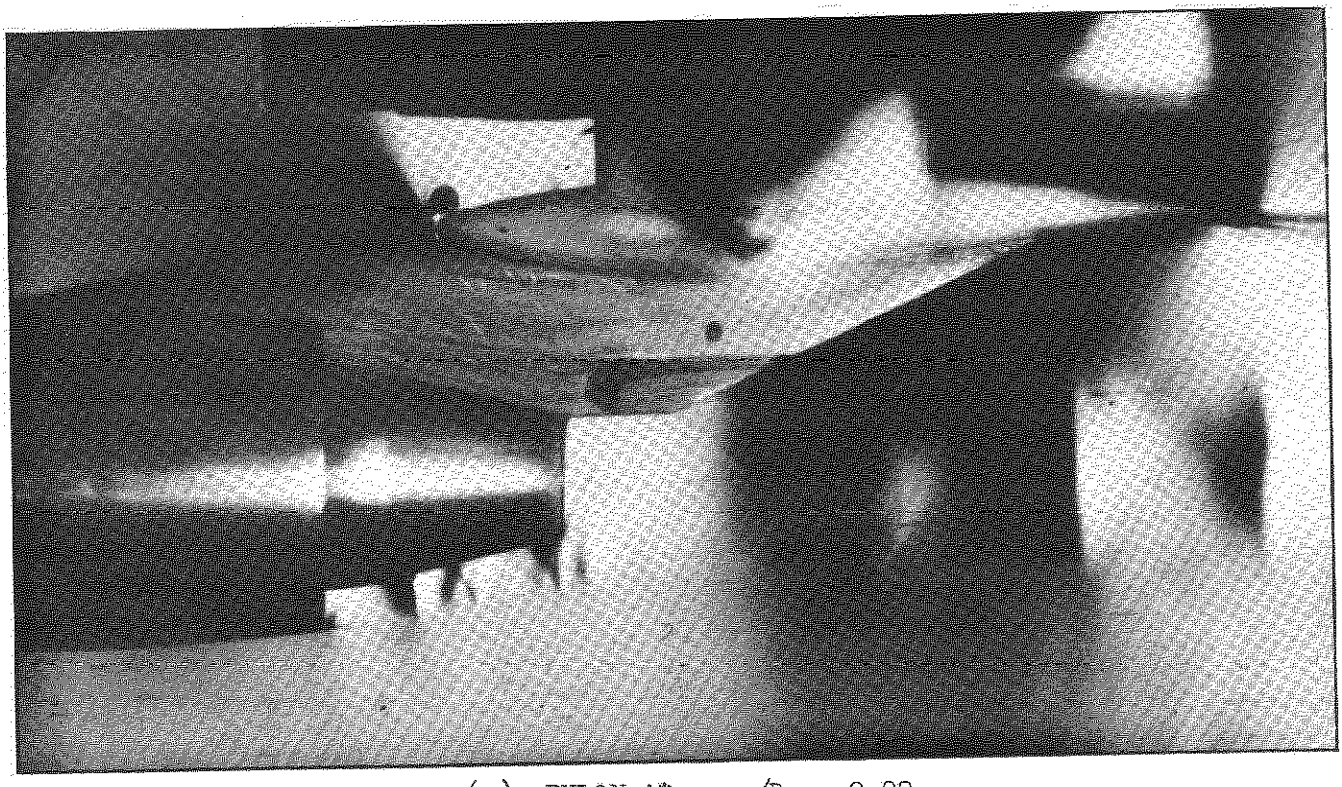

(a) PYLON A*: $z_n/D_e = 0{\cdot}29$

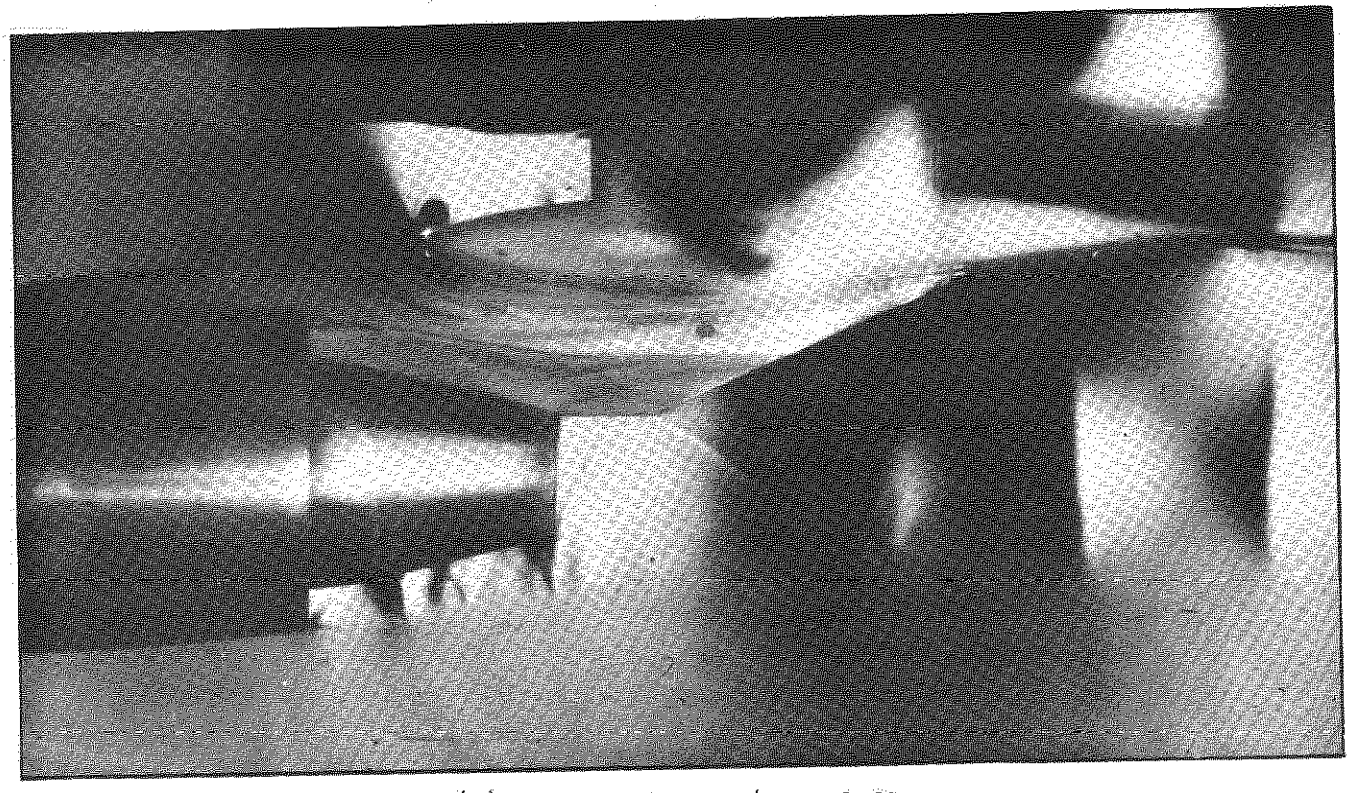

(b) PYLON B*: $z_n/D_e = 0{\cdot}23$

Fig.17 (a&b) Schlieren and oil-flow photographs with pylons

$x_n/D_e = 0{\cdot}38$, $H_j/p_o = 2{\cdot}65$, $M_o = 0{\cdot}72$, $\alpha = 0{\cdot}5°$

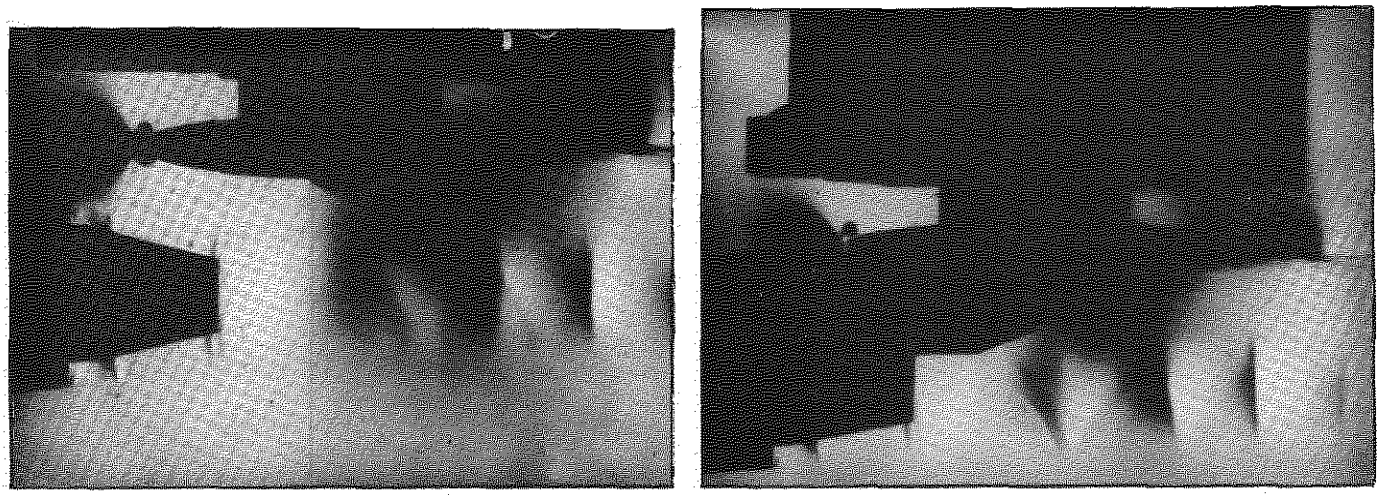

Schlieren knife-edge vertical

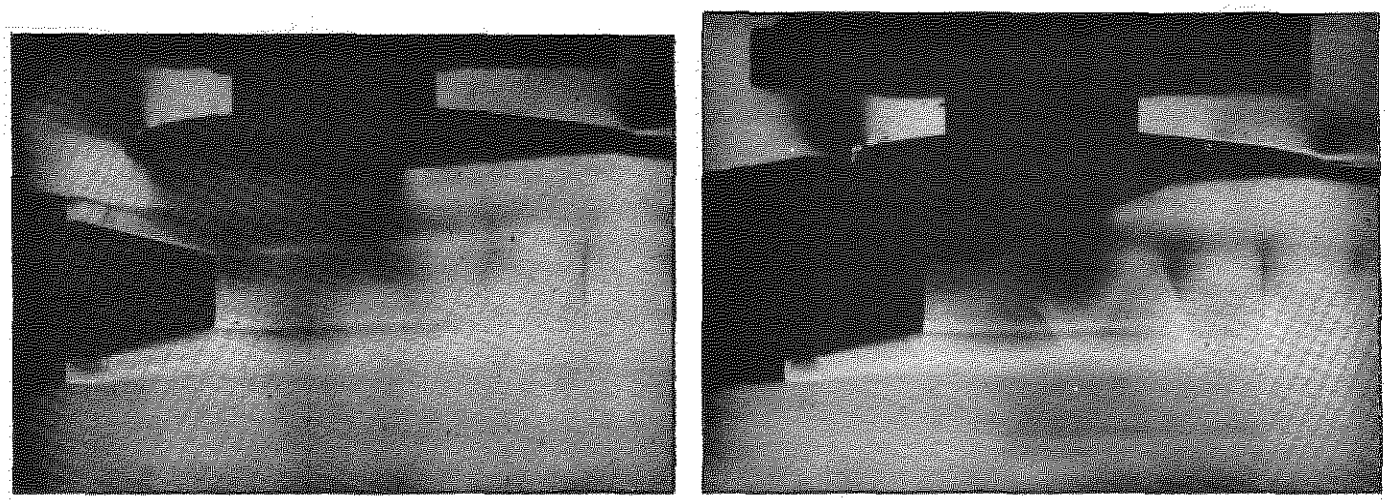

Schlieren knife-edge horizontal

WITHOUT PYLON: $\alpha = 0{\cdot}3°$ WITH PYLON: $\alpha = 0{\cdot}5°$

(a) JET FLOW WITH AND WITHOUT PYLON A* $H_j/p_o = 2{\cdot}4$

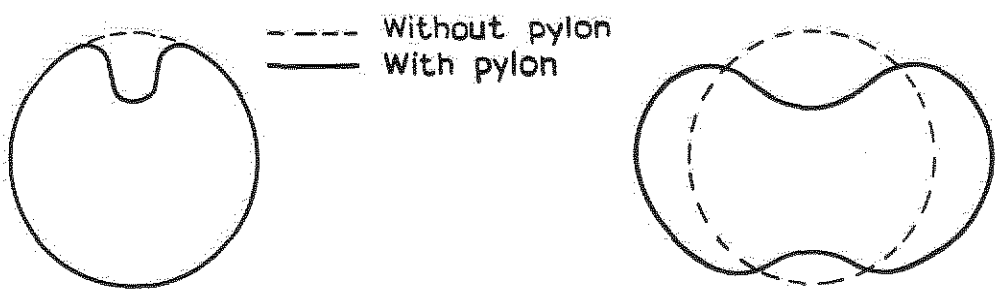

(b) HYPOTHETICAL JET CONTOURS

Fig.18 The effect on the jet stream due to the presence of a pylon

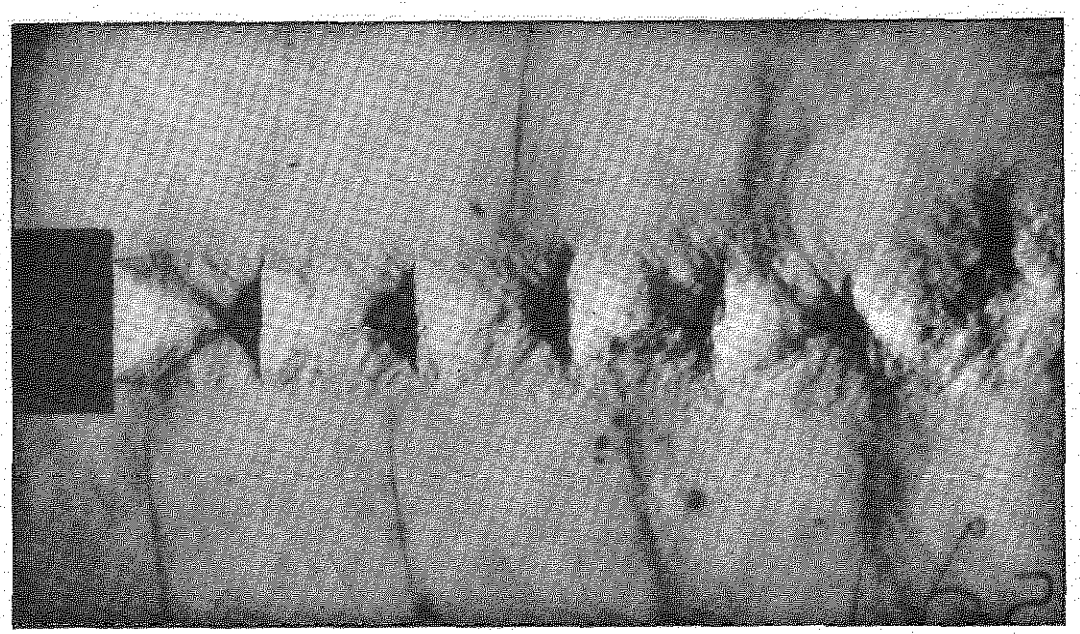

$M_o = 0{\cdot}50$: $H_j/p_o = 3{\cdot}03$

(a) Nozzle with annular base (Ref.5)

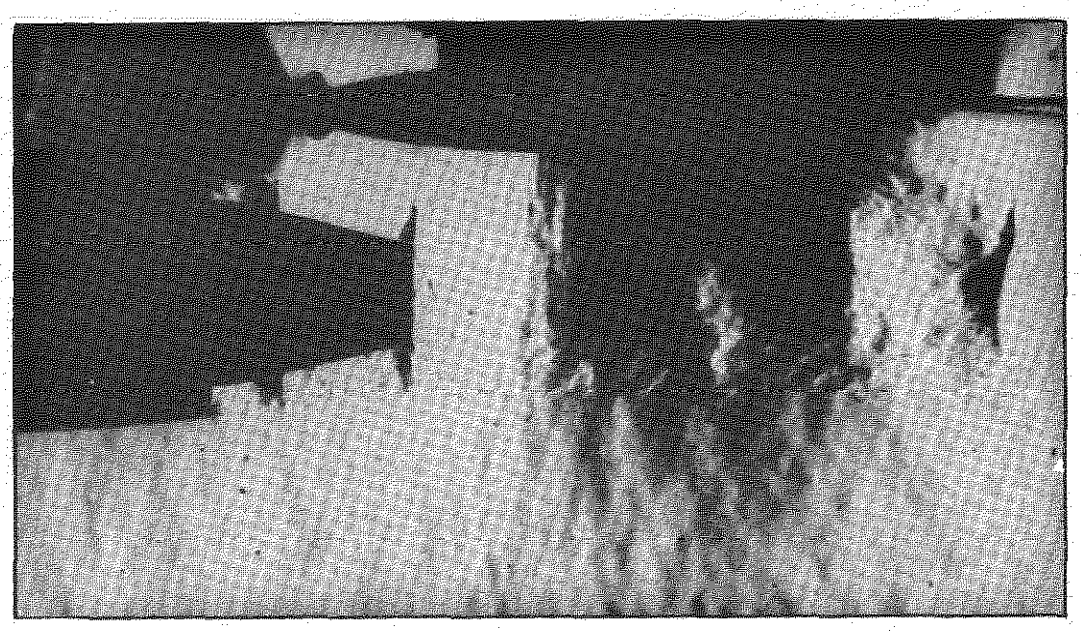

$M_o = 0{\cdot}72$: $H_j/p_o = 2{\cdot}65$

(b) Short nozzle and wing

Fig.19 (a&b) Schlieren photographs taken with a short duration spark

Printed in England for Her Majesty's Stationery Office by the Royal Aircraft Establishment, Farnborough. Dd.501371. K.4.

DETACHABLE ABSTRACT CARD

A.R.C. C.P. No.1156
April 1969

533.695.17
533.697.74
534.83

Kurn, A. G.

A FURTHER WIND TUNNEL INVESTIGATION OF UNDERWING JET INTERFERENCE

Further experiments, to investigate the interference of the jet stream issuing from a high bypass ratio engine mounted below a wing, are described

Tests have been made with a two-dimensional wing, and two nozzle shapes representing engines with different fan cowl lengths A jet blowing from these nozzles produced negligible interference on the wing upper surface However, a change in the lower surface pressure distribution occurred which was dependent only on the wing and nozzle geometry This interference was dominated by a high suction peak, which appeared to be related to a region in the jet where the alternate expansion and compression waves were not uniformly spaced

(Over)

A R C. C.P. No 1156
April 1969

533 695 17
533.697.74 :
534 83

Kurn, A. G

A FURTHER WIND TUNNEL INVESTIGATION OF UNDERWING JET INTERFERENCE

Further experiments, to investigate the interference of the jet stream issuing from a high bypass ratio engine mounted below a wing, are described

Tests have been made with a two-dimensional wing, and two nozzle shapes representing engines with different fan cowl lengths A jet blowing from these nozzles produced negligible interference on the wing upper surface However, a change in the lower surface pressure distribution occurred which was dependent only on the wing and nozzle geometry This interference was dominated by a high suction peak, which appeared to be related to a region in the jet where the alternate expansion and compression waves were not uniformly spaced.

(Over)

DETACHABLE ABSTRACT CARD

The tests were conducted mostly without an engine pylon. When a pylon was introduced the effect was reduced slightly, but the character of the interference remained unaltered

An attempt was made to show the possibility of a wing altering the noise level by reflecting the sound from a jet Schlieren pictures were taken with a spark source, but the expected phenomenon of aero-acoustic resonance was not found.

The tests were conducted mostly without an engine pylon When a pylon was introduced the effect was reduced slightly, but the character of the interference remained unaltered

An attempt was made to show the possibility of a wing altering the noise level by reflecting the sound from a jet Schlieren pictures were taken with a spark source, but the expected phenomenon of aero-acoustic resonance was not found

The tests were conducted mostly without an engine pylon When a pylon was introduced the effect was reduced slightly, but the character of the interference remained unaltered

An attempt was made to show the possibility of a wing altering the noise level by reflecting the sound from a jet Schlieren pictures were taken with a spark source, but the expected phenomenon of aero-acoustic resonance was not found

Published by
HER MAJESTY'S STATIONERY OFFICE

To be purchased from
49 High Holborn, London WC1 V 6HB
13a Castle Street, Edinburgh EH2 3AR
109 St Mary Street, Cardiff CF1 1JW
Brazennose Street, Manchester M60 8AS
50 Fairfax Street, Bristol BS1 3DE
258 Broad Street, Birmingham B1 2HE
80 Chichester Street, Belfast BT1 4JY
or through booksellers

C.P. No. 1156

SBN 11 470424 4